714563

Kligerman

1990

TRIUMF -- RESEARCH PROPOSAL	Dr. M. M. Kligerman, M.D. Los Alamos Scientific Laboratory P. O. Box 1663 Los Alamos, New Mexico 87544	Experiment no. Sheet 1 of 56 Field code

Title of proposed experiment NEGATIVE PION CAPTURE AND ABSORPTION on CARBON, NITROGEN, and OXYGEN

MES-200

Rec'd 6-27-72

Name of group Inland Northwest Nuclear Consortium

Spokesman for group H. B. Knowles, Washington State University

Members of group (name, institution, status)

P. A. Deutchman, University of Idaho, Assistant Professor of Physics

H. B. Knowles, Washington State University, Associate Professor of Physics

H. E. Sandberg, Washington State University, Assistant Professor of Biophysics and Physics

W. C. Sperry, Central Washington State College, Associate Professor of Physics

G. E. Tripard, Washington State University, Assistant Professor of Physics

REPOSITORY LANL/RC
COLLECTION Dir Off Files
BOX No. B-11, D-28
FOLDER MES 200 2/72-7/72

FILE BARCODE
00132860

COPIED FOR HSPT

H. B. Knowles
Department of Physics
WASHINGTON STATE UNIVERSITY
PULLMAN WASHINGTON 99163, U.S.A.

Date ready June 74	*Beam time requested (number of 8-hr. shifts)* *a) Parasitic* *b) As main user* 10

1093191

00132860.001

(Do not exceed one page)

Summary:

All meson factory accelerator installations are planning to attempt cancer therapy with negative pion beams. However, reported data on the nature and energy spectra of the heavy charged fragments emitted following pion absorption by the light nuclei carbon, nitrogen, and (particularly) oxygen are sparse, ambiguous, and to some extent, contradictory. More precise data are needed to obtain a real understanding of any clinical effects that will be observed. Additionally, in nuclear theory, more complete data on fragments from pion absorption are needed to advance our understanding of the structure of light nuclei.

Experiments are proposed to accomplish the following objectives:

(1) Measurement of the identities and spectra of the heavy charged fragments ejected following negative pion absorption in the elements C, N, and O. Fragments of very low range (<50 mg/cm^2) will be observed in a magnetic spectrograph. The energy resolution achievable is approximately 4%, exclusive of target thickness effects. Velocity-dependent variations of fragment charge states assist in removal of ambiguities. Fragments of medium range (50-800 mg/cm^2) will be detected in a range chamber. Here energy resolution is that corresponding to a 10 mg/cm^2 range interval. Data acquisition rates will be 1 to 2 events per second, permitting duplication in a few hours of all previously reported heavy fragment data from pion absorption on these nuclei.

(2) An autoparasitic experiment to measure the fractional capture ratios of negative pions on the C, N, and O atoms in tissue samples. This eliminates reliance on the questionable "Z-law" for pion capture and will supply needed information to the radio therapist. Pionic X-rays will be used for this purpose; the resulting precision is ± 10%.

Experimental area Meson Area

Primary beam and target (Energy, energy spread, intensity, pulse characteristics, emittance)

Energy - 450 MeV

Energy spread - no intrinsic requirement

Intensity - 400 μA

Pulse characteristics - 22.66 MHz repetition rate

Emittance - proton beam spot size 0.4 cm (no angle requirement)

Secondary channel Bio-Medical Channel

Secondary beam (Particle type, momentum range, momentum bite, solid angle, spot size, emittance, intensity, beam purity, target, special characteristics)

Particle Type - Negative Pion

Momentum Range - 126 to 132 MeV/c

Momentum Bite - ± 2.5%

Solid Angle - 10 msr

Spot Size - 3 x 3 cm

Emittance - As obtainable from channel with spot size requested ($x' \sim 8$ mr, $y' \sim 100$ mr)

Intensity - 2.3×10^7 π^-/s

Beam Purity - $e/\pi^- \leq 20\%$ (No other restrictions)

Target - following CH_2 absorber

0.8 mg/cm^2	Carbon, Melamine
10.0 mg/cm^2	Aluminium, Al_2O_3, (Other)
1 g/cm^2	Tissue Samples

COPIED FOR: 00132860.003

a) Scientific Value of the Experiment

The experiment has application to two entirely separate areas of scientific interest: 1) the use of negative pions in tumor therapy and 2) investigations in the structure of light nuclei. They may be conveniently considered in that order.

1) NEGATIVE PIONS IN RADIATION THERAPY

The application of negative pions to the irradiation of deep tumors has been considered since 1951[1-2] and has been a subject of steadily increasing interest since about 1961[3] when serious plans were first made for the construction of "meson factory" accelerators. Public presentations[4,5,6] and articles describing this concept for both general[7] and special[8] audiences have appeared so frequently in recent years that a detailed review would be gratuitous. In any event, all meson factories now under construction-LAMPF, TRIUMF and SIN-are being planned to include a medical radiation facility as an integral part of the beam area.

In common with all good medical practice, successful radiotherapy requires at least as much art as science, and committment to a trial of negative pions for radiation therapy of tumors is inevitable. Moreover, there are very positive prognoses for the use of negative pions in therapy. Studies of the energy deposition in a water phantom indicate a particularly favourable dose profile[9]. In addition, the work of Todd with heavy ions[10] and that of Raju[11] with weak beams of negative pions on human T-1 kidney cancer cells suggests a high probability of tumor destruction, even under the hypoxic conditions known to prevail in tumors. But it should be observed that the majority of studies on animal cell effects from particles of high ionization density--that is, particles having linear energy transfer (LET) in the vicinity of 1000 MeV-cm^2/g--have to date been done with T-1 cells: these cells can be readily grown and irradiated in vitro. Many other types of cells have been investigated in other contexts, but T-1 cells have been the principal

COPIED FOR HSDT 00132860.004

subject of the cell studies that relate to negative pion effects.

The work of Howard-Flanders has established the basic theoretical relation between the dimensions of the radiosensitive volume of the cell and the "most lethal value" of ionization density[12]. Cells of varying (radiosensitive) size may reasonably be anticipated in both malignant and normal tissues. It is eventually going to be important for the tumor therapy programme that the radiation sensitivity of many types of cells be better understood than at present. Perhaps more important than cell size, it will be necessary to understand the metabolic processes existing between different types of cells in a living organism and how damage to one type affects other types. If tumor destruction does occur under negative pion therapy, as hoped, it would still be useful for the paramedical worker to know the nature of the energy deposition in detail. Also, studies of the effects of negative pions in human tissue should properly encompass both somatic and genetic effects in healthy individuals who are employed at the meson-producing facilities, if the health physicist is to have the necessary information.

Such extensive studies of the radiosensitivities of specialized cell types are extremely difficult and are unlikely to be done in the near future. Damage to healthy cells can probably be safely estimated using the guidelines set forth by the International Committee on Radiation Protection[13]. The ICRP (in effect) has specified a value of <u>quality factor</u> (formerly: RBE) as a function of LET. The quality factor assumed is high and thus quite conservative. A more serious difficulty arises in the therapy program. Some tumors are quite likely to be radiation-resistant, possibly for rather complicated reasons related to the metabolic processes cited. In other instances, side effects from the radiations may be harmful to the patient. Comprehension of all effects, from the clinical and paramedical points of view, together with the need for protection of healthy personnel, will require that both of these things be known:

COPIED FC 00132860.005

(i) the relative proportion of negative pions that are captured on the various elements in tissue;

(ii) the fragmentation (decay) modes from each of these elements that result from nuclear absorption following negative pion capture--including branching ratios, particle species, and particle energy spectra.

The former problem turns out to bear on the latter, so it can be considered first. In 1947, Fermi and Teller postulated the "Z-law" for the relative capture proportions of negative mesons on the nuclei in chemical compounds: their estimate indicated that the capture probability per atom is proportional both to its atomic number, Z, and to its population[14]. It was also assumed that, in hydrogenous compounds such as hydrocarbons, the π^- or μ-mesonic hydrogen atom would become a small neutral particle and migrate until the meson was subsequently captured by a nucleus of higher atomic number. Thus the absorption reactions:

$$\pi^- + p \rightarrow \pi^0 + n$$
$$\rightarrow \gamma + n$$

are not anticipated in biological tissue. Both of these assumptions have been tested experimentally and the validity of the Z-law seems to be, at best, dubious. A rather complete review, showing the failure of the Z-law for both pions and muons has been presented by Kim[15], who stresses the importance of the nature of the chemical compound on relative capture probabilities. In the matter of pion capture on hydrogen, Ponomarev and Prokoshkin[16] point out that pion absorption on hydrogen in a compound may not be as unlikely as originally supposed, if molecular energy levels of the pion are taken into account.

Now, the actual ratios with which stopping pions are captured and absorbed on the nuclei of atoms in biological tissue is central to the pion radiotherapy program. Living tissue has the approximate composition $C_7N_2H_{70}O_{32}$[17] (muscle tissue is cited, but it is roughly representative of body tissues except for the

COPIED FROM 00132860.006

skeletal portions); cancer tissue seems to be chemically indistinguishable[18]. The probable ratio for pion capture on each of the various elements, in the light of the apparent failure of the Z-law, is somewhat uncertain--however, oxygen is clearly the most important element in this regard.

The data on fragmentation modes resulting from pion absorption in oxygen has been very difficult to obtain. A magnetic cloud-chamber study of fragmentation modes following capture of stopped pions in the gases ethylene and nitrogen (and helium) was reported by Ammiraju and Lederman in 1956[19]. This yielded data for charged particle emission from C and N that are almost unambiguous with respect to origin. (Oxygen gas, being paramagnetic, could not be studied by this technique). One of the early emulsion experiments using Ilford G-5 nuclear emulsions (composition: approximately $C_4NH_8O_2 \cdot AgBr$[20]) yielded information from 1038 stars from the light elements C, N and O, few of which could be absolutely distinguished as to origin[21]. The positive identification of oxygen events in emulsions remained a serious problem. In order to obtain more information for tumor therapy, Perkins and Fowler[22], and later, Fowler and Mayes[23], exposed wet (soaked) emulsions to pion beams (to enhance the oxygen fraction) and used corresponding dry emulsion data as a background for the wet emulsion events. The two studies were reported in the same publication[23] and presented 1344 events which were attributed to oxygen <u>on the basis of the correctness of the Z-law</u>. Soaking the emulsion caused it to swell and thus induced some severe limitations on precise observation of heavy recoils: nuclear fragments of charge greater than 1 could not be distinguished, and there was no mass discrimination: protons, deuterons and tritons were similarly undistinguishable from each other. In spite of these difficulties, an extremely careful and detailed analysis was done for each observed event and particular care was taken to identify such heavy recoils as would be associated with the $(\pi^-,2n)$ reaction and, especially, to compare the neutron

1093197

COPIED FC 00132860.007

multiplicity inferred from all events with that obtained from the independent neutron time-of-flight study of Anderson, et al[24].

Criticisms of these data are stated reluctantly, but the following facts need emphasis:

-- the number attributed to oxygen is based on background subtraction which is in turn based on a Z-law for capture that may be invalid;

-- fewer than 1400 events from pion capture, presumeably on oxygen, have been reported: these fall into a number of different categories and the statistical uncertainty on the important categories is 10% or worse;

-- the event ratio for wet/dry emulsions never exceeded 2:1--implying a "signal to background ratio" of 1:1 or less;

-- some charge assignments and most mass assignments are in some doubt;

-- α fragments up to about 50 MeV were reported but these should have been observed by Castleberry et al and the latter group reported no helium fragments[25].

-- supplementary interpretation of the dry-emulsion events, assigned to ^{12}C and ^{14}N capture, is not in good agreement with the virtually unambiguous cloud-chamber data[19].

The comments above are not intended to impugn one of the more ingenious and difficult nuclear physics experiments that has been performed with nuclear emulsions. The method itself imposes severe statistical limitations, and Fowler and his collaborators did as much with the emulsion events as could be expected. But, very few physics experiments have an extensive medical program based principally on their results. A peripheral difficulty that may be remarked is that the data of Anderson, et al,[24] are not in very good agreement with those of Hattersley, et al,[26] especially in the high-energy region.

1093198

00132860.008
COPIED FOR

The validity of the theoretical intranuclear cascade calculation of Guthrie, et al,[27] could be tested only by comparing it to the Fowler/Anderson data--with which its agreement is fair. The calculation predicted that a few percent of deuterons and tritons (in relation to protons) would be emitted following pion absorption on both ^{12}C and ^{16}O. The reality--as determined by subsequent experiment--is that the ratio of proton: deuteron: triton emission is approximately 3:2:1 for singly-charged particles of high-energy.[25] Clearly, much more data--especially on the nature and spectra of intermediate-mass and heavy charged particles emitted--is needed to develop a full understanding of negative pion radiology. The proposed experiment is designed to obtain such information.

2. NUCLEAR STRUCTURE FROM π^- ABSORPTION

The behaviour of the pion, once absorbed by the nucleus, has been a subject of speculation for some time. In 1951, Brueckner et al discussed two-neutron emission following absorption of a pion on an internal quasi-deuteron[28]. Ericson has developed this idea, indicating why two-nucleon emission is favoured (indeed, he asserts that single-nucleon emission is "forbidden") on the basis of energy and momentum conservation[29]. The significance of the energy spectrum and angular correlation of the neutrons in interpretation of the structure of a massive nucleus is discussed by Cheon[30]. Using various assumptions, calculations relating to spectra and angular correlation functions have been reported[31-35]. Both (2n) and (np) emission are considered although the former was theoretically expected to be favoured over the latter by a ratio, R, which is about equal to 3 because of the enhanced internal pairing of two unlike nucleons over that of two like nucleons; outgoing nucleon kinetic energies should be $\sim$ 70 MeV and the 2n or np pair should have its maximum correlation at about 180°. These predictions have, in the main, been verified in both counter[36-38] and sonic-chamber[39] experiments, although the measured value of the ratio R varies from about 3.3[37] to 5.1[36], and the n-n

COPIED 00132860.009

angular correlation is somewhat different from that of the outgoing n-p pair[37]. Neutron spectra from time-of-flight measurements[25,26] support the energy spectrum calculations, as do the proton spectra otherwise obtained[28]. But the high-energy nucleons show anomalies in their energy spectra which have stimulated calculations on the bases of more specific nuclear models: Sakamoto looked for effects from nuclear distortion in ^{14}N following π^- absorption[40] and his model does not forbid single nucleon emission. Spector, considering an ^{16}O target, also discussed the effects of nuclear distortion on both the incoming pion wave and on the emitted nucleons, and similarly found that single nucleon emission is possible[41]. Nguyen-Trung and Sakamoto have considered the internal correlation of the two nucleons before absorption and its effect on the energy spectra of the emitted nucleons[42]. There are a few experimental data supporting single-nucleon emission by π^- absorption[43], and some indirect support from observation of the (π^+,p) reaction[44]. (It has been suggested by Kopaleshvili and Machabeli that interactions of nuclei with absorbed stopped negative pions and with absorbed positive pions of about 100 MeV kinetic energy are very much alike[45].)

The above theory and experiment are applicable only to high-energy nucleon emission. The discovery of deuteron and triton emission from pion capture on ^4He by Schiff et al[46] initiated considerable theoretical and experimental work on absorption on " α- clusters" in light nuclei. The most complete theoretical studies reported on helium itself are those of Ammiraju and Biswas[47] and Eckstein[48]. Eckstein found a high probability for triton emission ($\sim$ 20%), in contrast to the result of Ammiraju and Biswas, but in agreement with experiment[46]. Extension of the model to include pion absorption on α -clusters in light nuclei has been the basis of several theoretical studies relating to deuteron and triton emission from ^{12}C and ^{16}O[49-54]. Cheon has also included the final-state interaction between the two emitted nucleons when negative pions are absorbed on carbon[55].

COPIED FOR 00132860.010

The extensive experiments performed with stopped pions in nuclear emulsions (where ^{12}C is a major constituent) have increased the interest in this nucleus[56-63]. When adequate charge and mass discrimination was possible, emulsion studies have tended to support the emission of deuterons, tritons, α-particles, and other multi-nucleon fragments following negative pion absorption on a light nucleus. In fact, Rabin et al[57] reported the emission of deuterons and tritons from light elements in nuclear emulsions almost a decade before they were confirmed by the sonic spark chamber observations of Castleberry, et al[25]. Beyond the intrinsic problems of identifying the capturing nucleus and fragment charge discrimination, the utility of emulsion data is limited in practice by the number of events that can be analyzed, as remarked[21-23]. Experiments using counters have been somewhat more successful than emulsion experiments in producing data in which the pion-initiated events are unambiguous as to origin, are sufficiently numerous to be statistically significant, and have satisfactory mass resolution[27,64-66]. The difficulty with most counter experiments that have been reported to date is that thick targets must be used because of the low intensities of existing pion beams. Presumably particles of low range are emitted but not detected. The integral range spectra presented by Fowler and Mayes[23] indicate that about half of the charged particles from pion absorbtion do not go beyond about 5μm (1 mg/cm^2) in emulsion. The use of target thicknesses on the order of several grams per square centimeter prohibits detection of most of the charged particles.

One other light nucleus--^6Li--has been the subject of intensive theoretical and experimental work because of its expected (α + d) internal cluster structure. Sakamoto has considered the (π^-,2n) reaction, based on an harmonic-oscillator ^6Li model[67]; Baus and Fuld have corrected this model for its barycentric motion[68]; Cheon has considered internal rescattering[69]; and others have examined ^6Li, varying the theoretical assumptions in different ways[70-73]. Experimental studies indicate that two-neutron emission is indeed the dominant mode of fragmentation[37,66,74-76].

COPIED FC00132860.011

But the studies do not agree on many particulars. The marked suppression of triton emission reported by Cohen, et al[74] contrasts with the result of Castleberry, et al[74], who find that a triton is the most common isotope to be emitted from ^{6}Li following pion absorption. The importance of fragment identification from ^{6}Li, with relation to an understanding of the structure of ^{12}C and ^{16}O, arises from the result that capture on a deuteron cluster is apparently favoured over capture on an alpha cluster. The rather large branching ratios for triton emission from carbon and oxygen nuclei thus poses a suggestion of strong α- clustering within their structures.

At the present writing, the following assertion about negative pion absorption in light nuclei may be made: the reported data are insufficiently precise to guide the theory. There are indeed internal conflicts--e.g. Calligaris et al[66] report neutron spectra from ^{6}Li which do not agree with those reported by Nordberg et al[37]. The proportion of the fragmentation mode: $^{14}N(\pi^-,3\alpha)$ seen by Fowler and Mayes is in conspicuous disagreement with that reported by Lederman and Ammuiraju, and the discrepancy is discussed by the former authors at some length. Some of these difficulties may arise from uncritical acceptance of the Z-law, while others may originate from observation of events which are actually caused by pions whose kinetic energies are as high as several tens of MeV--resulting from the necessary use of thick targets. (In spite of the theoretical similarities suggested between fast and stopped pions[45], they may in fact differ). However, the principal experimental problems seem to be inadequate statistics and poor fragment identification.

The physically interesting processes related to radiative pion absorption (π^-,γ) and single-charge-exchange (π^-,π^0) have not been considered, although these processes may leave the residual nucleus excited to the giant resonance[77]. Radiative pion absorption appears to have a branching ratio[77] of about 10^{-2}, while single-charge-exchange has a branching ratio of less than 10^{-4} in light nuclei[78]. These processes are of secondary importance, at least when compared to the two-

1093202

COPIED F 00132860.012

nucleon, several-nucleon and heavy-particle fragmentation modes. The two-nucleon mode is expected to account for about 40% of the total[37], while the extant emulsion data on ^{16}O interactions indicates that branching ratios of 5 to 20% obtain for the other nucleon and heavy fragment modes[23].

The analysis of heavy-fragment emission from all light nuclei following π^- absorption will be considerably improved by the use of the apparatus proposed here.

b) Description of the Experiment

1) GENERAL DESCRIPTION

It seems appropriate to propose the use of the TRIUMF Pion Medical Channel to perform this experiment because of its value to the negative pion therapy programme. The medical channel has been described by Harrison[79] and by Witten[80]; there is also a record of correspondence between W. Sperry and G. Jones discussing its use for stopped pion and muon physics experiments[81].

General principles on which the experiment have been designed are these:

-- Because no single apparatus can yield all the information desired, double (and occassionaly, triple) targets are employed in the stopped pion beam, for reasons of economy of beam time;

-- Therefore it is mandatory that the targets be sufficiently close to each other so that pion beam losses by capture and, especially, multiple scattering, do not materially inhibit successful performance of other experiments "downstream", but on the other hand, components are adequately isolated from each other so that secondary particles from one apparatus do not simulate primary events in another;

-- In view of the intense (distributed) source of fast neutrons ($\sim 7 \times 10^7$ n/s) that arises from negative pion capture in targets, detectors and absorbers along the pion beam line, it is necessary that all detectors used be either neutron-insensitive, or remote and well-shielded, or capable of

COPIED FOR 00132860.013

being "rejuvenated". (Thus, plastic scintillators, sodium iodide scintillators, and conventional solid-state detectors cannot be used near the beam line);

-- The especially favourable time structure of the TRIUMF beam will be exploited as much as possible. At a pulse repetition rate of 22.66 MHz, assuming 5 proton pulses per cycle and near -isochronism of pions entering the system, pions will arrive in pulses about 44 ns apart. There will be initially very few pions in each pulse, and various losses will reduce their number to less than one per 44 ns, thus permitting individual pions to be traced through the absorber-detector-target system ("inspected") at a rate of a few million per second. (An experiment with comparable restrictions at the LAMPF facility could inspect only about 250,000 pions per second because of the 6% LAMPF rf duty factor.)

-- The electronic logic and analog systems have been designed with existing "off the shelf" equipment in mind. It is believed that more compact and economical systems can be created. However, the present design establishes feasibility.

A simple block diagram of the proposed detection system is shown in Fig. 1. The pion beam, focused to about 3 x 3 cm^2, is slowed by a thick absorber. Individual pions are counted and located by beam-line detectors C_1, and C_1', which are of the multiwire proportional counter (Charpak) type. Target T_1 is an extremely thin (800 $\mu g/cm^2$) target, viewed by a magnetic spectrograph. Detector C_2 is an intermediate Charpak beam-line detector, preceeding target T_2 (about 10 mg/cm^2) which is viewed by a range chamber. Detector C_3 is, again, a Charpak beam-line detector. Intermittently, a third thick target T_3 will be set at the end of the detector, using beam-line detector C_4 to serve as a verification counter for pions

COPIED F00132860.014

stopping in T_3. The details of each detection system will be described more fully below.

2) BEAM CHARACTERISTICS

A negative pion beam will be extracted at an energy of 50 MeV with a momentum interval of ± 2.5%. This pion energy was tentatively selected on the basis of factors described in the Final Report of the Yale Design Study: production cross-section, acceptance solid angle, and decay-in-flight are included, although nuclear attenuation is so small for pions of this energy that it may be ignored[82]. Cross section data used were those of Lillethun et al, which were selected because they most nearly compare to the TRIUMF proton energy and angle[83]. The following assumptions were additionally made:

primary proton energy:	450 MeV
primary proton current:	400 μA
pion production target:	18 g/cm^2 Be

Using the above values, an independent calculation yielded a stopping density of pions given by

$$\frac{dn}{dR} = 1.6 \times 10^7 \ \pi^- \ -(\mathrm{cm}^2/\mathrm{g\text{-}s})$$

which is in excellent agreement with the stopping densities obtained by both Harrison[79] and Witten[80] for a ± 5% momentum interval. The selected momentum interval of ± 2.5% leads to a FWHM range variation of 1.45 g/cm^2, which must be appropriately modified by the intrinsic range straggling width of 0.23 g/cm^2 (range values in this section are quoted in carbon). The number of pions stopping somewhere in the system every second has the value:

$$\frac{dn}{dt} = 2.3 \times 10^7 \ \pi^-/\mathrm{s}$$

When this number is divided by the pulse frequency, it is seen that the average number of pions entering the system every 44 ns is almost 1.0 π^-/pulse. Such a

COPIED FROM 00132860.015

rate (if unattenuated) would be too high for individual pion inspection, because the probability of receiving two or more pions in one pulse would be about 24%. However, multiple scattering attenuates the rate by a factor of between 4 and 5, as will be described below, and reduces the rate of plural events to a few percent, while reducing the rate of the desired single pion traversals by only about one-half. It is probably not profitable at this time to calculate pion yield and rates in more detail until empirical values are obtained from measurements on the channel itself: adjustment to the desired rate can be obtained by variation of the momentum interval.

The distribution of pions in range is deduced to be approximately uniform, because the reported production cross section increases with pion energy near 50 MeV[83], while the stopping power, (-dT/dx), decreases with energy in an approximately compensatory manner. The calculated range distribution of pions is shown in Fig. 2. The thinner targets are located in the region of maximized stopping density, that is, at values of total range in carbon between 10.0 and 10.8 g/cm^2. In practice, CH_2 will be used for the primary absorber because it produces less multiple scattering than carbon.

The number of particles actually stopping in each of the targets is obtained in the following manner: the lateral spread of particles stopping <u>in a given target</u> is principally determined by the thickness of the target itself because that is the measure of the highest pion energy that will stop there. Other factors are the thickness of the preceeding beam-line detectors, absorbers, and targets and their distances from the target in question. Because a broad momentum interval is injected into the system, all pions will not be characterized by the same mean-square scattering, $\langle\theta^2\rangle$, at the same target. To determine scattering losses, one starts with pions of energy corresponding to mean range in the target and calculates how much scattering occurred in the thickness of the

COPIED F00132860.016

previous detector, thus obtaining the root-mean radius increment $\Delta\langle r^2\rangle$ from that detector by the relation:

$$\Delta\langle r^2\rangle = \langle\theta^2\rangle \ell^2$$

(where ℓ is the detector-target separation). The calculation goes backward in a stepwise manner to the position where the beam enters the primary absorber, where $\langle r^2\rangle$ is taken to be 3 cm^2 (derived from 3 x 3 cm^2 beam spot). Then at each location, the ratio of $\langle r_0^2\rangle$ to the cumulative sum:

$$\langle r^2\rangle = \langle r_0^2\rangle + \Delta_1\langle r^2\rangle + \Delta_2\langle r^2\rangle + \ldots$$

is the reduction factor for a beam stopping in a given target.

Multiple scattering of the pions was readily calculated by employing one of the formulae developed by Rossi[84]:

$$\langle\theta^2\rangle = \frac{E_0^2}{c^2}\,\frac{1}{X_0}\int_{p_1}^{p_2}\frac{1}{-\beta^2\left(\frac{dp}{dx}\right)}\,\frac{dp}{p^2}$$

for pions slowing from momentum p_2 to p_1 (where E_s = 21 MeV and X_0, radiation length), because the reciprocal of $\beta^2\left(-\frac{dp}{dx}\right)$ could be represented by a simple analytic form. Using this equation, and the specific dimensions and detector/target thicknesses shown in Fig. 3, the reduction factors for the stopping densities at each target and detector are as shown. Even at C_1, the reduction factor is calculated to lie between 3 and 4, because of the scattering in the primary absorber. The stopping-density reduction factors thus obtained imply the same areas for all targets and detectors between the primary absorber and C_4.

The calculated <u>average</u> reductions at the various targets and detectors do not prohibit obtaining information about individual pions, because beam-line particle inspection by suitably designed Charpak counters removes much uncertainty as to both direction and location of individual pions. Statistical uncertainty applies to the lateral displacement induced in the last leg the pion traverses before

1093207

COPIED FOR HSPT 00132860.017

stopping. Particular care had to be taken for this reason in the case of the magnetic spectrograph target, because the root-mean-square lateral distance through which the pion is scattered as it strikes the target becomes the effective target width, which in turn influences the resolution of the spectrograph. For the design shown, rms width at the T_1 target is about 0.75 cm.

Range-energy data for the scattering calculations were drawn from the extensive tabulations by Rich and Madey[85]. Other (unpublished) data for pion ranges at very low energy have been used.

When slowly-moving pions are to be stopped in a thin target, two special and closely related concerns are, first, whether they will survive decay-in-flight when moving between the last detector and the target, and second, whether pions of somewhat higher energy that do penetrate the target (but lose energy in traversing it) will survive to be recorded in the succeeding beam-line counter. The succeeding counter is used to set a logic "veto" on preceding phenomena, as will be described. Two factors common to both problems lead to a favourable answer. First, the uniform distribution in range does not imply a uniform distribution in kinetic energy--the energy spectrum of pions that emerges from any object must vary as the reciprocal of the stopping power and the emergent pions are thus biased toward higher energy-dramatically so, because it is the pions of lowest energy (up to 1 MeV) that are of interest. Second, decay is in itself not serious, pion losses to decay being of the order of only 20% in the case of the thinnest target if preceeded by a 5 cm drift space. These properties are not by themselves sufficient to lead to uncritical reliance on the efficiency of the veto counter. However, the decay product of the pion is a muon, which has a minimum kinetic energy of 1 MeV and a minimum range of 150 mg/cm^2. The muon is readily projected forward if there is any appreciable pion velocity. It is therefore estimated that a veto counter following a thin pion-stopping target will be from 95 to 98% reliable, the value depending to some degree on geometry. Since its basic purpose is to

COPIED FOR 00132860.018
UCBT

1093208

permit distinction between real and background events, its reliability can be checked in situ by elementary techniques.

A final concern is that of beam contamination. The estimates of Sperry[81] indicate that nucleons and electrons will appear in the following ratios:

$p/\pi \approx 0.1$ $\qquad$ $n/\pi \approx 0.06$ $\qquad$ $e/\pi \approx 0.2$

The protons of momentum equivalent to that of 50 MeV pions have less than 10 MeV and will easily be stopped in the primary absorber. The neutrons are presumably of thermal or epithermal energies (in order to have negotiated two 45° bends) and are certainly a less serious problem than fast neutrons arising from the stopped pions themselves. The 20% electron contamination is a greater obstacle. If electrons arise from the production target they are momentum-equivalent to the pions and thus have about 128 MeV kinetic energy. They are not readily scattered but are highly penetrating, and thus must lead to some undesired responses in the beam-line detectors. An ideal solution is not immediately evident, but probably discrimination against pulses of minimum ionization in the beam-line detectors will be sufficient.

Muon contamination is also present, both from decay of stopping pions and also from pion decay in the medical channel. Fast muons arise because only about 7% of the injected 50 MeV pions survive the trip through the 7m channel and the forward-decaying mesons are nearly momentum-equivalent to the pions. But, even a quadrupole channel specially designed to trap muons from pions decaying in flight rarely exceeds 5% in efficiency.[86] Typical muon contaminations in other pion beams suggest that 0.1% capture efficiency is a reasonable estimate for the medical channel. Thus, a μ/π ratio of about 0.1 is anticipated. Such muons have (before passing through the primary absorber) a kinetic energy of about 60 MeV and a range of 15 g/cm^2. They will be exceedingly difficult to distinguish from pions by pulse discrimination and will probably trigger the beam-line detectors at the ratio

COPIED FC 00132860.019

of one muon per 10 pion events. However, if a nuclear event should be caused by a captured muon, it must be a weak-force interaction which is commonly a two-body reaction, e.g.,

$$\mu^- + {}^{12}C \rightarrow {}^{12}B + \nu_\mu$$

The appearance of monoenergetic heavy fragments can thus be used to estimate the effect and magnitude of muon contamination. From the radiobiological point of view, of course, it is absolutely necessary that muon absorption effects on nuclei be measured along with those of the pions.

3) DETECTOR SYSTEMS

(i) X-Ray Detector

This system is discussed first because of the importance of its results to subsequent weighting of decisions. A preliminary experiment using this system alone could be defended.

It has been indicated that the knowledge of actual pion capture ratios on various elements in tissue is uncertain. It appears that measuring the proportions of low-level pionic X-rays would be the least ambiguous method of determining ratios. This will work very well for tissue samples which are principally of (CNOH) composition, but additional data on Ca and P pionic capture X-rays will be needed to extend the study to bony tissue.

An excellent recent review paper by Backenstoss[87] summarizes much of what is known about pionic X-rays, and some of this information is excerpted and presented in Table I. The low yields of electromagnetic radiation from the 2p-1s transitions are caused by competitive processes that permit deexcitation of the upper levels: nuclear absorption, and, to a lesser extent, Auger processes. The shortness of the lifetimes of the pionic states is reflected in the widths of the lines, which principally result from the widths of the lower levels. No absolute yield values

COPIED FOR 00132860.020

Table I

Pionic X-Rays from Selected Nuclei

Capturing Nucleus	Transition	Energy (keV)	Line Width (keV) (lower level)	Yield (%)
^{12}C	2p-1s	93.19±0.12	2.96±0.25	7.6±0.9
^{14}N	2p-1s	124.74±0.15	4.48±0.30	6.8±0.8
^{16}O	2p-1s	159.95±0.25	7.56±0.50	4.9±0.7
^{27}Al	3d-2p	87.53±0.10	0.11±0.08	Not reported
^{31}P	3d-2p	116.78±0.10	0.20±0.08	Not reported
^{40}Ca	3d-2p	209.66±0.18	2.29±0.13	Not reported

(In this table, the values of highest reported precision have been selected. There are other values reported.)

1093211

COPIED FOR 00132860.021

for the higher (3d - 2p) transitions are reported, although Backenstoss describes how these can be obtained. Energy calibration can be done with muonic X-rays, which are always present.

The equipment to be used to view a tissue sample of about 1 g/cm^2 thickness is a high-purity (intrinsic) germanium detector. A conventional Ge(Li) detector would not survive the intense fast neutron flux to which it must be subjected. However, the intrinsic germanium detector can be repeatedly recycled from liquid nitrogen temperature to room temperature, thus permitting annealing away most of the radiation damage sustained. A detector of this type is now commercially available: it is reported that energy resolution comparable with that of a Si(Li) X-ray detector is achieved (e.g., 470 eV FWHM at 122 keV) but with much higher detection efficiency (on the order of 50% at 100 keV)[88]. Currently manufactured models of the Ge detector have only 30 mm^2 active area, but this restriction may improve in the next year or two. The analysis of the X-rays from the detector will proceed by a conventional preamplifier-amplifier system feeding a multichannel analyzer. A pileup rejection system will be included to maintain energy resolution in the presence of the high neutron flux. The analyzer will be gated by a $11'23\bar{4}$ event and will require about 30 μsec to process an X-ray count. Thus, a basic limit on the rate of analysis is about 3 x 10^4 events per second, but this is not the most severe limitation. In practice, it will be necessary to keep the active area of the detector at least 10 cm from the thick tissue target because of the need to interpose about 10 g/cm^2 of material of very low atomic number in order to keep the high-energy protons arising from nuclear absorption of pions out of the detector. The detector solid angle is thus estimated to be about 3.3 msr. Even using a thick target, multiple scattering, as seen, reduces the number stopping in it to about 2.5 x 10^5 π^-/s. The resultant estimate of data accumulation for 2p-1s transitions is about 2.5 events/sec. The minimum requirement on total counts for any single sample appears to be approximately 10^5 counts on transitions of interest,

COPIED FOR 00132860.022

because of the extraordinary backgrounds that arise in pion/muon capture experiments. An operating time of 8 to 10 is thus indicated for every tissue sample. It is at present uncertain whether this period will exceed the time that the detector can receive exposure to a fast neutron flux before it must be warmed and rejuvenated: rough calculations suggest that such deterioration may start after a period of 5 to 6 hours.

It is reemphasized that this experiment is parasitic to the charged-particle detection experiments and could profitably be run as a separate experiment, at a higher data rate.

(ii) Secondary Charged-Particle Detection Systems

The light elements of interest in the initial medical application--carbon, nitrogen and especially, oxygen--are the subject of primary importance in these experiments. The only data available on oxygen is that of Fowler and Mayes[23], if we except the high-energy proton-deuteron-triton data of the University of Virginia group[25]. The expected fragments and their energies can be roughly estimated from these data. (The older cloud-chamber[19] and emulsion[21] data were also considered in the instances of nitrogen and carbon.) Some estimates of average and maximum kinetic energies, principally based on the Fowler-Mayes data, appear in Table II. Here, maximum kinetic energies of fragments are derived from simple kinematic considerations, while average values are those given by Fowler and Mayes. The list of fragments is almost certainly incomplete; Vanderhaeghe and Demeur assigned about 4% of their light-element pion capture events in emulsion to ^{8}Li fragments[21]. The latter were distinguishable from their characteristic "hammer tracks"; Li^{8} is by no means an unexpected fragment, on the basis of isospin conservation.

The broad spread of species and kinetic energies of fragments indicates that a single detection system would be inadequate. The maximum ranges of the fragments vary from 2.61 mg/cm^2 (in the case of ^{14}N) to 170 mg/cm^2 for the most energetic

COPIED FOR 00132860.023

Table II

Average and (Calculated) Maximum Kinetic Energies of Several Nuclear Fragments from Pion Absorption on Carbon, Nitrogen and Oxygen

Fragment	Carbon		Nitrogen		Oxygen	
	Tavg (MeV)	Tmax (MeV)	Tavg (MeV)	Tmax (MeV)	Tavg (MeV)	Tmax (MeV)
^{14}N	-	-	-	-	5.8	14.4
^{12}C	-	-	•	18.0	6.3	25.8
^{11}B	*	*	*	23.5	5.0	27.4
^{10}B	4.7	18.5	*	•		39.0
^{9}Be		26.0	*	•	4.6	42.2
^{7}Li	8.0	35.5	*	*	5.4	44.0
^{6}Li		52.1	*	*		62.0
^{4}He	*	76.5	*	84.2	*	78.0
^{3}He	*	*	*	*	*	*
^{3}H	*	~ 80	*	*	*	~ 80
^{2}H	*	~ 80	*	*	•	~ 80
^{1}H	*	~ 90	*	*	*	~ 90

• Not reported

COPIED FOR 00132860.024
HGPT

^{4}He fragments, even if the hydrogen isotopes (which have ranges up to almost 10 g/cm^2) are excluded from consideration. Indeed, if the particles are classified in terms of range (here quoted in aluminium, from the data of Northcliffe[89]) three distinguishable domains of range are perceived:

-- high range, 800 mg/cm^2 to 8.0 g/cm^2

-- medium range, 50 mg/cm^2 to 800 mg/cm^2

-- low range, 1.0 mg/cm^2 to 50 mg/cm^2

The group at the University of Virginia has performed many of the useful measurements in the high-range domain[25]. It does not seem profitable to repeat their experiments, especially knowing that some extensions of this work are planned at LAMPF in the near future. It is hoped that collaborative efforts on interpretation with members of this group can be pursued. It has therefore been decided to concentrate experimental efforts in the low-range and medium-range domains.

(ii) A) Low Range Domain

In this domain are found virtually all of the fragments of $A < 6$ and presumably also the lighter fragments of extremely low energy. At least two independent measurements must be performed on any nuclear fragment to obtain its energy and its identity. Consideration of the various techniques indicated that two of them could not be employed with heavy fragments: stopping power (because of low penetration and scattering) and time-of-flight (because of lack of time discrimination at any distance commensurate with adequate detector solid angle). The classical method of measuring magnetic rigidity together with kinetic energy emerged as the sole practical candidate although it initially seemed that certain ambiguities might appear in this method. Reconsideration of the processes dispelled this concern, for the reason to be described.

Heavy particles moving through media have a rapidly changing charge state. This has been shown by Northcliffe to be a function of the ratio, ξ, of the

COPIED FOR HSPT 00132860.025

particle velocity, v, to the "Bohr velocity" of the electron in the 1s orbit of the fragment:

$$\xi = \frac{137v}{Zc}$$

where Z is the atomic number of the fragment[89]. Several discrete charge states coexist and the fragment charge, on emergence from a target, is likely to have any of these several discrete values, which occur in a predictable ratio as a function of ξ. Thus, ^{12}C fragments emerging from a target with 10 MeV kinetic energy have a value of ξ about equal to 1.0. Therefore that the ^{12}C fragments must appear in the following proportions:

20% in the Z-state	(^{12}C VI)
48% in the (Z-1) state	(^{12}C V)
27% in the (Z-2) state	(^{12}C IV)
5% in the (Z-3) state	(^{12}C [redacted])

Each of these four charge states of 10 MeV ^{12}C fragments will appear at quite different values of magnetic rigidity--^{12}C VI at 258 kG-cm, ^{12}C V at 310 kG-cm, ^{12}C IV at 389 kG-cm and ^{12}C III at 516 kG-cm. Fragments of lower kinetic energy have lower values of ξ and, consequently, tend to have lower charge states, while those of higher kinetic energies are completely ionized or in the (Z-1) charge state. The effects are, first, to concentrate the heavy fragments in a relatively narrow spread of magnetic rigidity, and second, to provide certain useful redundance of information. For example, the fragments ^{3}He II and ^{12}C IV have essentially identical magnetic rigidities when they have the same kinetic energy but a parallel determination of the unambiguous spectra of the charge states of ^{12}C V and ^{12}C [redacted] permits calculation of the ^{12}C IV spectrum and thus allows it to be subtracted from the combined spectrum.

Figure 4 shows a plot of the magnetic rigidity, $B\rho$, against the kinetic energy, T, for a number of expected heavy fragments. The lines have been terminated either

COPIED FOR HSPT 00132860.026

at their maximum kinetic energy (shown in Table II) or when the fractional ratio of that charge state falls below (arbitrarily) 20%. Thus, the ^{12}C VI line extends between 10 MeV and 26 MeV.

The pattern of the lines on Fig. 4 indicates that most of the important feasible measurements on low-range particles can be done in the region of magnetic rigidity between 200 kG-cm and 800 kG-cm. A magnetic spectrograph with energy-sensitive and position-sensitive detectors set along the focal plane is the obvious method to use. The line separation on Fig. 4 also suggests a lower limit on the desired minimum of energy resolution, $\Delta T/T$, compatible with particle identification. The two lines that most nearly overlap are those for ^{11}B IV and ^{6}Li III, and an energy resolution of 1.6% would be needed to distinguish between these fragments. (The lines of Fig. 4 represent relations between T and $B\rho$ <u>after</u> the particles have left the target, and while the target thickness inevitably causes severe distortion of the original energy spectra, fragment type discrimination is a separate reason for reducing energy resolution as much as possible.) It will be seen that this stringent resolution requirement cannot be met, because of target width influence, but all other particle separations impose only a 4% requirement on energy resolution, which can be achieved.

The spectrograph is in many ways very similar in its requirements to one needed at a tandem Van de Graaff installation. A number of broad-range high-resolution spectrographs were investigated. Among these were the Enge split-pole spectrograph[90] now in use at the University of Pittsburgh[91] and its sophisticated descendant, the QD^3 spectrograph described by a group at Chalk River[92]. Such spectrographs are obviously too elaborate for an experiment which basically needs only a few percent of energy resolution. Consideration of the properties of alternate designs of simple uniform-field spectrographs has been presented by a group from the Copenhagen Institute for Theoretical Physics[93]. A version of their final design, shown in Fig. 5, was ultimately selected. The "Copenhagen" spectrograph

COPIED FO 00132860.027
HSDT

is not double-focusing although the positive angle of incidence causes some vertical convergence and thus leads to a satisfactory value of detector solid angle (Fig. 6a). It is corrected for second-order aberrations in the radial plane and, for the design parameters selected, has a typical energy resolution of less than 1% (Fig. 6b). Its particular virtue for the present application lies in its relatively small value for the effect of target width on the resolution (Fig. 6c), which is of the order of 0.25% per mm of target width. In this experiment (unlike one using a conventional accelerator) it is not possible to control the lateral beam spread precisely, because of the scattering in the C_1' detector*. Collimation would lead to serious background from pions stopping in the collimator. The 0.75 cm width from scattering in C_1' induces an energy resolution about 3.7%, which is within the desired limit for energy resolution. The 800 $\mu g/cm^2$ T_1 target is entirely compatible with the lowest heavy-particle energies that can be measured with the spectrograph.

The magnetic spectrograph will use position- and energy-sensitive semiconductor detectors in the focal plane. A spatial resolution of 0.5 mm is easily obtained with the 10 mm x 50 mm Nuclear Triodes that are currently available[94]. The solid angles shown in Fig. 6a are calculated using the 10 mm dimension. Counting rates of 10^4 to 5×10^4 random counts per second per detector could be handled readily although the anticipated rates will be considerably below this value. Sixteen detectors will be arranged as in Fig. 7 in order to cover the desired region of the focal plane completely.

A block diagram for four detectors is shown in Fig. 8. This is representative of the system plan for sixteen detectors. (The logic which determines that a single event took place and a pion stopped in the target is described below.)

---

* Alternatively, the T_1 target could be reduced in width to produce the desired resolution, at the cost of a substantial loss in counting rate.

COPIED FOR HSPT 00132860.028

The signals Energy, Position, and Detector will be gated into a small local computer. The computer will then be appropriately interfaced with CAMAC.

The 16 Nuclear Triodes were selected for depletion depth according to their location, by comparing maximum particle ranges to their magnetic rigidities. An array that will stop virtually all particles of energies below 15 MeV (other than protons) consists of: 4 detectors of 60 micron thickness,

4 detectors of 120 micron thickness,

8 detectors of 240 micron thickness,

in order from lowest to highest radius. Some particles which have ranges higher than the corresponding depletion depths may be to some degree susceptible to analysis by comparison of their stopping power with the magnetic rigidity[95].

The magnet itself has pole tips 93 cm x 30 cm in dimension and a 2.5 cm gap. It is to be operated at 16 kG maximum field, a field slightly in excess of the linear region but one allowing maximum constriction of the detector array. A choice of a lower value for maximum field would improve the variation in resolution with target width and some other parameters (although not detector solid angle) but a weaker field would cause the spectrograph and its attachments to become excessively large. The proposed magnet will expend about 8 kW of regulated power, and requires about 200 kg of copper winding to maintain the field. The weight of the yoke, pole tips and support is estimated to be 7 metric tons.

With the geometry and detector as planned, the value of stopping pion density is about 3×10^6 π-cm^2/g-s at T_1. The number of pions stopping and being captured in the 1.1 g/cm^2 (projected) thickness is thus 3.3×10^3/s. The solid angle used in this estimate is based on the representative average kinetic energies of the fragments (Table II). Their average magnetic rigidity, as shown in Fig. 4, is about 300 kG-cm. The average solid angle is thus taken to be 6 msr: on these assumptions the average counting rate is 1.6 heavy fragments per second.

COPIED FOR
HSPT 00132860.029

1093219

The T_1 target will be slightly smaller than the 3 x 3 cm^2 assumed, so the actual count rate in the spectrograph will be about 1 heavy fragment per second. This seems to be extremely low. However, with only 20 minutes of operation at this rate, as many events will be counted as were measured in the entire Fowler-Mayes experiment. Between 3 and 4 hours of operation will provide as much usable data as has been reported, cumulatively, from all emulsion and cloud-chamber studies of π^- absorption on light nuclei. It will also in general be possible to identify the nucleus of origin with no ambiguity. At least one 8-hour run, permitting the acquisition of data on 30,000 heavy fragments, is tentatively requested for each of the several targets of interest.

(ii) B Medium Range Domain

It is seen from Fig. 4 that some light fragments have magnetic rigidities in excess of 800 kG-cm. Also, some of the light fragments having suitable radii within the spectrograph still exceed the thickness of the particular Nuclear Triode they strike. It would be uneconomical and in some instances, impossible to use a detector of sufficient thickness to detect all particles. Therefore a rather elementary range-chamber detector is used to obtain data on fragments in the medium-range domain.

This detector records information that to some degree overlaps data obtained from the spectrograph. It consists of a stack of 10 proportional counters, each of about 10 mg/cm^2 thickness, as seen in Fig. 9. These are <u>not</u> Charpak counters--all of the wires in any one detector element are connected together. The range chamber is in fact simply a 10-channel version of the differential range counters extensively employed some 20 years ago for charged particle detection and analysis in the presence of high neutron backgrounds.

The range chamber is designed with a somewhat constricted (3 cm) front aperture in order to allow for multiple scattering of the heavy fragments, as

1093220

COPIED FOR HSPT 00132860.030

they are slowed in the absorber foils between detectors. It is, provided with remotely insertable preabsorbers of 100 mg/cm^2, 200 mg/cm^2, and 400 mg/cm^2, in order to permit measurement of fragments having total ranges up to 800 mg/cm^2. The range chamber views the T_2 target (set at 45° to the pion beam) at a distance of 10 cm. It is not maintained in a vacuum, because the air thickness is comparable to the range resolution desired. (A helium-filled bag may be used in the pion beam to reduce scattering.)

Such a detector is only capable of determining the energy (range) and the atomic number, Z, of any fragment, but not the isotopic species. It does not, for example, distinguish between ^{6}Li and ^{7}Li fragments, a few of which might have sufficient range to enter the range chamber. It is anticipated that overlapping data on isotopic mass, obtained from the upper end of the spectrograph, will provide the necessary guidance for identification of such fragments.

Contingent upon the receipt of a $11'2\bar{3}$ enabling gate from the beam-line detectors, the range chamber is interrogated and a record of the sizes of these pulses that arise from the deepest detector in the detector stack are recorded if coincidence among all previous detectors is observed. Thus, after the $11'2\bar{3}$ signal, the presence of an $ABCDEF\bar{G}$ signal from the range chamber will force the recording of counter pulses E, F. If all counters record, the last two detector pulses will be recorded. The electronics associated with the range chamber appear in Fig. 10.

It is calculated that about 3.3×10^4 π^-/s will stop in the T_2 target. The solid angle of the range chamber to the target is 70 msr, indicating a nominal counting rate of about 160 counts/s. The rate does not exceed the capability of any part of the system. The majority of the entering particles will be high-energy hydrogen isotopes and these may tend to obscure the detection of heavier fragments. In that case, selective discrimination against acceptance of the smaller pulses induced by hydrogen fragments in the first few detectors will eliminate the problem.

1093221

COPIED FOR HSPT 00132860.031

It is actually anticipated that only about 10% of the fragments stopping in the range chamber will fall within the medium-range domain of interest, perhaps about 10 events/s. However, these will be to some extent distributed among the 8 possible combinations of variable preabsorber range. Thus the projected rate of data accumulation is on the order of 2 counts/s. This may be compared with the expected rate from the magnetic spectrograph: an 8-hour run on a given target with the spectrograph will produce comparable statistics on data from the range chamber while it is being operated in conjunction with the spectrograph.

(iii) Beam Line Detectors

Multiwire proportional counters ("Charpak counter") will be used to count the individual pions in the beam. These proportional counters have been described elsewhere[96] and are selected because of their comparatively limited response to neutron and gamma radiation. The detectors each have their wires arranged vertically (at about 2 mm spacing in the case of detectors C_1 and C_1') in order to identify position and direction of the pion stopping in the T_1 target, thereby improving the momentum resolution of the magnetic spectrograph. A time resolution of 30 ns can be achieved by choosing the appropriate gas mixture and voltage. Counting rates of the order of 10^7/s have been reported[97]. This means that two pions resulting from consecutive beam pulses will be distinguishable in time. The C_1' counter will be made very thin by using windows of Formvar films (50 $\mu g/cm^2$) covering a molybdenum mesh[98]. Gas pressures of over 1 atmosphere can be sustained by such films although much lower pressure differentials are expected to be employed.

Fig. 11 shows the electronics which determine that a pion has stopped in the T_1 target and the associated logic which records its trajectory. Detectors C_1, C_1', and C_2 consist of 16-wire proportional counters. A signal in detector C_2 causes an event from the spectrograph to be rejected. When a $11'\bar{2}$ signal occurs, the number of the wires in the corresponding detectors are encoded and transferred to the CAMAC interface. This information is then available to the on-line computer

COPIED FOR 00132860.032
HSDT

if a charged particle is detected in the spectrograph within the appropriate time limit. A similar system is employed for identifying a stopping event in either the T_2 or T_3 targets. The fundamental reason for using beam-line detectors is the elimination of background by the verification procedure described.

4) TARGETS

In order to investigate the light elements of immediate interest, it is tentatively planned that the T_1 and T_2 targets will be fabricated as described.

Carbon: This is quite straightforward, because targets in the 0.5-10 mg/cm^2 range can be produced by evaporation or (in this application) from CH or CH_2 foils.

Nitrogen: The standard material used for thin solid nitrogen targets is melamine ($C_3N_6H_6$) which can be successfully used for stopping pions, especially after carbon targets have been investigated. Melamine has certain hazards associated with its use (especially if it is overheated)[99] and alternate targets are being considered. A gas target may be preferable for T_2.

Oxygen: Conventional organic compounds, such as mylar, tend to be relatively oxygen-poor. One satisfactory approach to fabrication of a thin solid oxygen target has been the use of Al_2O_3 foils (prepared by anodization) together with the determination of the background from the aluminium. It is virtually impossible at this time to predict which heavy fragments will arise from negative pion absorption by Al: hopefully the (π^-2n) or (π^-(np) modes will be dominant and permit a relatively unrestricted picture of the oxygen-absorption fragments in the spectrograph and range chamber. However, there are alternatives--one extreme example might be a gaseous O_2 target between thin sheets of Formvar--and these will continue to be investigated. The T_2 target could readily be a gas target. One very interesting possibility for the T_1 oxygen target is the use of a water

COPIED FOR
HSPT 00132860.033

fogging device, similar to the type developed by Lane for the environmental control stage in electron microscopy[100]. This must necessarily be used with a vacuum pump made to handle condensable materials.

Others: Of next greatest importance to the radiobiological problem are the elements Ca and P. Because these elements are not assigned top priority in the first phase of this experiment, the fabrication of targets has not been seriously considered. Deposition of Ca and P compounds on carbon, aluminium, beryllium or other suitable thin carrer foil may be a simple solution provided that the fragment background from the carrier element has previously been measured.

c) Experimental Equipment

A tentative list of equipment is submitted with the following qualifications:

(i) The electronics are listed on the assumption that mostly shelf items will be used. It is believed that considerable economy in these items can be achieved by internal redesign.

(ii) The equipment that may be available at TRIUMF is not known to us at present.

(iii) Some of the equipment is now available at one of the participating institutions. It is hoped that some cooperation will develop with colleagues in Canada, who may have or be able to obtain the use of other components.

(iv) It is planned that major equipment fabrication and testing will be done principally at Washington State University, where availability of shop facilities a 2 MeV accelerator, PDP-15 computer, etc., will permit basic checkout before removal to Vancouver. No important use of the TRIUMF shops is envisioned at this time.

Equipment List	Comment
Beam Line Detector System	
5 x Charpak detectors	
80 x amplifiers, triggers, delays, monostables, and gates	

1093224

COPIED 00132860.034

5 x OR gates

5 x 5 MHz scalars

1 x NIM bin

2 x encoding matrices

(1 x CAMAC-PDP-15 interface) — for checkout at WSU

Magnetic Spectrometer

16 kG magnet, 7T, 30 x 93 cm^2

8 - 10 kW DC power supply (0.1% reg) — Needs: 10 kW;7.5 gpm water

vacuum tank, vacuum system

16 x Nuclear Triodes

32 x ORTEC 121 preamp

16 x ORTEC 114 preamp power supply

4 x ORTEC 210 detector control

32 x Tennelec TC 211 linear amplifiers

3 x NIM bin

32 x Tenn. TC 620 Stretcher-multiplexer
4 x Tenn. TC 420 Multiplexer-controller
2 x Tenn. TC 501 ADC
7 x Tenn. DB 100 Special Bins
CAMAC Interface
} Multiplexing Equipment

Range Chamber

10 x ORTEC 121 preamp

5 x ORTEC 114 preamp power supply

10 x Tenn. TC 211 linear amplifier

10 x ORTEC 489 delay amplifier

18 x ORTEC 426 linear gate

1 x ORTEC 484 25 kHz scalar

2 x Tenn. TC 501 PHA

2 x NIM bins

Some of these are available or obvious substitutions can be made

COPIED FOR
HSPT00132860.035

1093225

X-Ray Spectrometer

Detector GE 411-1 (inc. preamp)	Vertical model
1 x Bias Supply	all of this equipment available at participating institutions
1 x RC shaper	
1 x Linear amplifier w/ baseline restoration	
1 x Pileup rejector	
1 x 2056 multichannel analyzer	
1 x Scalar (25 kHz)	
1 x NIM-bin	

Miscellaneous

Equipment racks	req. of TRIUMF
200 x (2" x 4" x 8") concrete blocks-shielding	req. of TRIUMF

A scale drawing of the proposed installation is shown in Fig. 12.

d) Readiness

(Dates assume major support initiated Feb. 1973)

Charpak detector:	design and construction	2/73 - 8/73
	testing and modifications	9/73 - 10/73
	logic testing at WSU	12/73 - 4/74
Electronics:	redesign	2/73 - 6/73
	construction	7/73 - 2/74
	testing	2/74 - 5/74
Magnet:	design	2/73 - 4/73
	fabrication	5/73 - 8/73
	measurement and correction	9/73 - 1/74
Vacuum System and Spectrograph:	design	4/73 - 6/73
	fabrication	6/73 - 10/73
	vacuum testing	11/73
	counter installation	12/73 - 3/74
	counter testing at WSU	3/74 - 5/74
Range Chamber:	design	2/73
	fabrication	3/73 - 4/73
	counter testing	5/73 - 6/73
	logic testing at WSU	7/73 - 10/73
Targets:	fabrication	6/73 - 8/73
	(testing of gas cells)	9/73 - 10/73

1093226

COPIED FOR 00132860.036
HSPT

It is believed that the above schedule can be met with the addition of 1 post-doctoral fellow, 3 to 4 half-time graduate students to the group. Professor Deutchman may continue some theoretical studies with the aid of one graduate student during construction.

e) Machine Time Required

The core of the experiment is the spectrograph, with its rate of 1 count/second the projected count rate of the range chamber count rate is 2 counts/second. The X-ray detection experiment should (in principle) be initiated first in order to determine the appropriate weighting of subsequent time. In performing the Al_2O_3-Al subtraction, and the melamine-carbon subtraction, it will be necessary to make decisions on time allocations on the basis of the information obtained. A provisional projection of time needed is presented here:

Block	No. of Shifts	T_1, T_2	T_3	Purpose
I	2	C	tissue	alignment , shielding
II	2	C,Al	tissue	recheck , C
III	3	Al_2O_3,Al	(Al_2O_3?)	O subtraction
IV	3	Melamine (C)	--	N subtraction

It is requested that Block II should follow Block I by 2 weeks, with a similar interval between Blocks II and III. Blocks III and IV can be together.

f) Data Analysis:

The electronics will be assembled and tested using the facilities of the Nuclear Radiation Center at WSU. These facilities include a PDP-15 computer which has 16K of memory, magnetic disk storage, 2 DEC tapes, line printer, card reader, and oscilloscope display. Part of the proposal is to obtain an interface to CAMAC for this PDP-15 so that the electronics can be pretested at WSU in detail. Since the PDP-15 is non-portable, it is hoped that an on-line computer similar to the PDP-15 will be provided by TRIUMF and have its own interface to CAMAC. If none of the on-line computers at TRIUMF are from DEC, some programming assistance will also be required.

1093227

COPIED FOR HSPT 00132860.037

References

1. Unpublished Memorandum by R. D. Hill and others, University of Illinois, ca 1951.

2. Discussion between C. Richman and C. A. Tobias, ca 1952. Reported in; C. Richman and M. R. Raju, UCRL-18806 (Sept. 1969).

3. P. H. Fowler and D. H. Perkins, Nature 189, 524 (1961).

4. Presentation by H. Batho, British Columbia Cancer Institute, TRIUMF Users' Meeting, Boulder, Colo., October 1969, Vancouver, B. C., May (1969).

5. Presentation by H. Kaplan, Stanford University Medical School, LAMPF User's Meeting, Boulder, Colo., October 1969.

6. K. Goebel, Z. Naturforsch. 219, 1808 (1966).

7. P. H. Fowler: 1964 Rutherford Memorial Lecture; Proc. Phys. Soc. 85, 1051 (1966).

8. L. Rosen, Nuclear Applications 5, 379 (1968).

9. S. B. Curtis and M. R. Raju, Radiation Res. 34, 239 (1968).

10. P. Todd, Radiation Res. Supp. 7, 196 (1967).

11. M. R. Raju, unpublished. This work is cited in P. Todd, LA-4653-MS (January 1971) "The Prognostic Value of Cell Studies in Evaluating New Accelerator Beams for Therapy" which is perhaps the most complete recent published review of the proposed pion radiotherapy program.

12. P. Howard-Flanders, Adv. Med. Biol. Physics 6, 553 (1958).

13. U. S. National Bureau of Standards; Tech. Bulletin No. 41, 17 (1957).

14. E. Fermi and E. Teller, Phys. Rev. 72, 399 (1947).

15. Y. N. Kim, "Mesic Atoms and Nuclear Structure" (North-Holland, Amsterdam, 1971) pp 5-17.

16. L. I. Ponomarev and Yu. D. Prokoshkin, Comments on Nuclear and Particle Physics, 2, 176 (1968).

17. W. A. Gibson, ORNL-TID-61-6-48 (1959) p. 5.

18. R. J. Winzler, "The Physiopathology of Cancer" (Ed.: F. Homburger and W. H. Fishman, Harper and Bros., New York, 1953) Ch. II 18, p. 168 ff.

19. P. Ammiraju and L. Lederman, Nuovo Cim 4 (Ser. X) 238, (1956).

20. P. Demers, "Ionographie" (Montr. Univ. Press, Montreal, 1958) p. 85.

1093228

COPIED 00132860.038

21. G. Vanderhaeghe and M. Demeur, Nuovo Cim. 4, (Suppl), 932 (1956).

22. P. H. Fowler and D. H. Perkins, private communication to one of us (HBK) March 7, 1963. Professors Fowler and Perkins most courteously provided a rough analysis of their early data, some of which was later included in Ref. 23.

23. P. H. Fowler and V. M. Mayes, Proc. Phys. Soc. (London) 92, 377 (1967).

24. H. L. Anderson, E. P. Hincks, C. S. Johnson, C. Rey and A. M. Segar, Phys. Rev. 133, B392 (1964).

25. P. J. Castleberry, L. Coulson, R. C. Minehart and K. O. H. Ziock, Physics Lett. 34B, 57 (1971).

26. P. M. Hattersley, H. Muirhead, and J. N. Woulds, Nucl. Phys. 67, 309 (1965).

27. M. P. Guthrie, R. G. Alsmiller, Jr., and H. W. Bertini, Nucl. Inst. Meth. 66, 29 (1968).

28. K. A. Brueckner, R. Serber and K. M. Watson, Phys. Rev. 81, 575 (1951); Phys. Rev. 84, 258 (1951).

29. T. Ericson, Phys. Lett. 2, 278 (1962).

30. Il-T. Cheon, Nuc. Phys. 79, 651 (1966).

31. P. Huguenin, Nuc. Phys. 41, 534, (1963).

32. J. M. Eisenberg and J. Letournaux, Nucl. Phys. B3, 47 (1967).

33. Il-T. Cheon, Phys. Rev. 155, 900 (1967).

34. H. J. Weber, Ann. Phys. 53, 93 (1969).

35. T. I. Kopaleishvili, Sov. J. Nucl. Phys. 1, 686, (1955).

36. S. Ozaki, R. Weinstein, G. Glass, E. Loh, L. Neimala and S. Wattenberg, Phys. Rev. Letters 4, 533 (1960).

37. M. E. Nordberg, K. F. Kinsey and R. L. Burman, Phys. Rev. 165, 1096 (1968).

38. F. Calligaris, C. Cernigoi and I. Gabrielli, Nucl. Phys. A126, 209 (1969).

39. D. M. Lee, R. C. Minehart, S. E. Sobbotka, and K. O. H. Ziock, Bull. Am. Phys. Soc. (Ser. II) 1684 (1970).

40. Y. Sakamoto, Nuovo Cim. 53B, 433 (1966).

41. R. M. Spector, Phys. Rev. 134, B101 (1964).

42. C. Nguyen-Trung and Y. Sakamoto, Nucl. Phys. B1, 139 (1965).

43. A. T. Varfolomeev, Soviet Phys. JETP 8, 373 (1959).

1093229

COPIED FOR USDT 00132860.039

44. T. R. Witten, M. Blecker and K. Golow, Phys. Rev. 174, 1166 (1968).

45. T. I. Kopaleishvili and I. A. Machabeli, Physics Letters 22, 181 (1966).

46. M. Schiff, R. H. Hildebrand and C. Giese, Phys. Rev. 122, 265 (1961).

47. P. Ammiraju and S. N. Biswas, Nuovo Cim. 17 (Ser. X) 726 (1960).

48. S. C. Eckstein, Phys. Rev. 129, 413 (1961).

49. I. S. Shapiro and V. M. Kolybasov, Soviet Phys. JETP 17, 185 (1963).

50. N. S. Zelemskaya, Yu. F. Smirnov and N. P. Yudin, Bull. Acad. Sci. USSR, Phys. Ser. 29, 184 (1966).

51. V. M. Kolybasov, Sov. J. Nuc. Phys. 3, 704 (1966).

52. N. F. Golovanova, N. S. Zelemskaya and N. El-Nagar, Nucl. Phys. A113, 1 (1968).

53. T. I. Kopaleishvili and I. Z. Machabeli, Sov. J. Nucl. Phys. 12, 525 (1970).

54. V. M. Kolybasov and V. A. Tsepov, Sov. J. Nucl. Phys. 14 (1971).

55. Il-T Cheon, Phys. Letters 26B, 549 (1968).

56. J. P. Massue, H. Braun, G. Baumann and P. Cüer, J. Phys. 24, 841 (1963).

57. N. V. Rabin, A. O. Vaĭsenberg and É. D. Kolganova, Phys. Lett. 2, 110 (1961).

58. A. O. Vaĭsenberg, É. D. Kolganova and N. V. Rabin, Sov. Phys. JETP 20, 85A (1965).

59. Y. A. Batusov, S. A. Bunyatov, V. M. Sidorov and V. A. Yarba, Phys. Lett. 22, 487 (1966).

60. V. I. Petrukhin, Yu. D. Prokoshkin and A. I. Fillipov, Sov. J. Nucl. Phys. 5, 229 (1967).

61. V. G. Kirillov-Ugryumov, F. M. Sergeyev and A. I. Fesenko. Sov. J. Nucl. Phys. 5, 604 (1967).

62. Yu.A. Batusov, S. A. Bunyatov, V. M. Sidorov and V. A. Yarba, Sov. J. Nucl. Phys. 6, 834 (1967); Sov. J. Nucl.Phys. 7, 20 (1968).

63. N. M. Agabian, Yu.A. Batusov, S. A. Bunyatov, Kh. M. Chernev, P. Cüer, J. P. Massue, V. M. Sidorov and V. A. Yarba, Proc. 3rd International Conf. on High-Energy Physics and Nuclear Structure, (Plenum, New York, 1970) p. 449.

64. K. O. H. Ziock, C. Cernigoi and G. Gorini, Phys. Letters 34B, 471 (1970).

1093230

COPIED FOR HSPT 00132860.040

65. D. M. Lee, R. C. Minehart, S. E. Sobottka and K. Ziock, Bull. Am. Phys. Soc. 15, (Ser. II) 1684 (1970).

66. F. Calligaris, C. Cernigoi , I. Gabrielli and F. Pellegrini, Proc. 3rd International Conf. on High-Energy Physics and Nuclear Structure (Plenum, New York) p. 367

67. Y. Sakamoto, Nucl. Phys. 87, 414 (1966).

68. M. Baus, M. Fuld, Bull. Acad. Roy. Belg. Sci. 54, 294 (1968).

69. Il-T. Cheon, Nucl. Phys. A121 679 (1968).

70. Y. Sakamoto, Nuovo Cim. 37, 774 (1965).

71. T. I. Kopaleishvili and I. Z. Machabeli, Sov. J. Nucl. Phys. 4, (1968).

72. G. Alberi and L. Taffara, Nuovo Cim. 58B, 441 (1968).

73. B. F. Jain and B. Bannerjee, Nuovo Cim. 69A, 419 (1970).

74. R. C. Cohen, A. D. Kanaris, S. Margolis and J. L. Rosen, Phys. Letters 14, 242 (1965).

75. H. Davies, H. Muirhead and J. N. Woulds, Nucl. Phys. 78, 663 (1966).

76. F. Calligaris, C. Cernigoi, and I. Gabrielli, Nucl. Phys. A126, 209.

77. V. I. Petrukhin and Yu. D. Prokoshkin, Nucl. Phys. 54, 414 (1964); Nucl. Phys. 66, 669 (1965).

78. V. I. Petrukhin, Yu. D. Prokoshkin and A. I. Filippov, Soviet J. Nucl. Phys. 5 229 (1967).

79. R. W. Harisson, VPN 71-7.

80. T. Witten, VPN-70-21.

81. W. Sperry, Memorandum 3 Sept. 1970; G. Jones, Letter 17 Sept. 1970; W. Sperry Letter 2 Oct. 1970.

82. Yale Study on High-Intensity Proton Accelerators, Internal Report Y-12 (Yale University, October 1964) p. IV-172, ff.

83. E. Lillethun, Phys. Rev. 125, 655 (1962).

84. B. Rossi, High Energy Particles (Prentice-Hall, New York, 1952) p. 66

85. M. Rich and R. Madey, UCRL-2301, 1954.

86. Ref. 82, p. IV-203.

COPIED FOR 00132860.041
UCDT

87. G. Backenstoss, Proceedings of the Third International Conference on High-Energy Physica and Nuclear Structure, 1969 (Ed. S. Devons, Plenum New York-London, 1970) p. 469 ff.

88. Preliminary Bulletin: GE/S.T.P.(71-1), General Electric Co., Space Technology Products, P. O. Box 8349, Philadelphia, PA, 19101, U.S.A.

89. L. C. Northcliffe, Ann. Rev. Nuc. Sci. 13, 67 (1963); L. C. Northcliffe and R. F. Schilling, Range and Stopping Power Table for Heavy Ions, TAMVEC Report, (Texas A and M University, College Station, Texas, 1965).

90 J. E. Spencer and H. A. Enge, Nucl. Instr. Meth. 49, 181 (1967).

91 W. W. Daehnick, Phys. Rev. 177, 1763 (1969).

92 J. C. D. Milton, G. C. Ball, W. G. Davies, A. J. Ferguson and J. S. Fraser, A High Resolution, Broad Range Spectrometer for the MP Tandem, AECL-3563, 1970.

93. J. Borggreen, B. Elbek and L. Perch Nielsen, Nucl. Instr. Meth. 24, 1 (1963).

94. W. W. Daehnick, Guide to the Selection and Use of Position-Sensitive Detectors (Nuclear Diodes, Prairie View, Illinois, 1969).

95. Lynn B. Brown and H. B. Knowles, Phys. Rev. 125, 1339 (1962).

96. G. Charpak, R. Bouclier, T. Bressani, J. Favier and Č. Zupančič, Nucl. Instr. Meth. 62, 262 (1968).

97. C. Grunberg, L. Cohen, and L. Mathieu, Nucl. Instr. and Meth. 78, 102 (1970).

98. R. J. Grader, R. W. Hill, C. W. McGoff, D. S. Salmi, and J. P. Stoering, Rev. Sci. Instr. 42, 465 (1971).

99. N. I. Sax, Dangerous Properties of Industrial Materials, (2nd Ed. Rheinholt, New York and London, 1963) p. 961.

100. W. C. Lane, Proc. of the 3rd Annual Scanning Electron Microscope Symposium, (IIT Research Inst., Chicago, 1970) p. 41 ff.

1093232

COPIED FOR HSPT 00132860.042

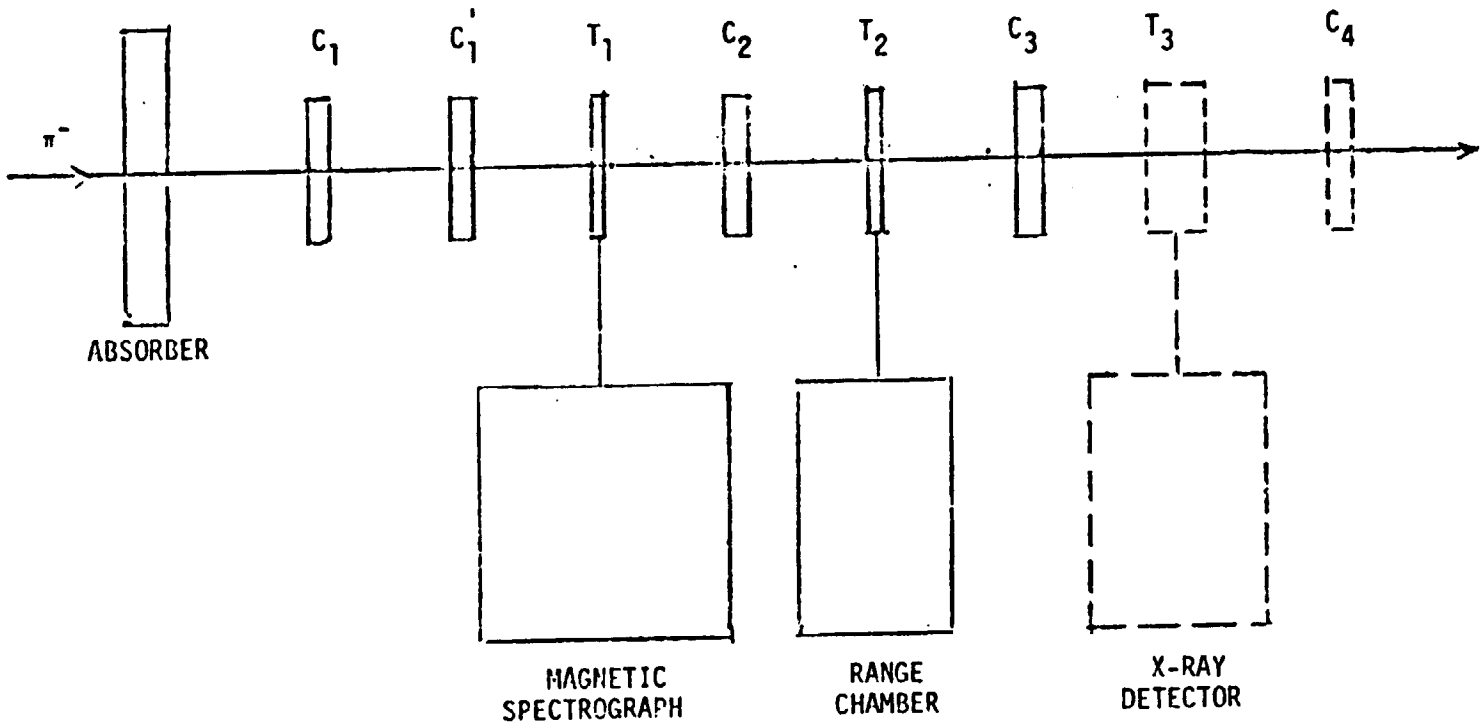

Fig. 1. BLOCK DIAGRAM OF DETECTION SYSTEM

COPIED 00132860.043
1093233

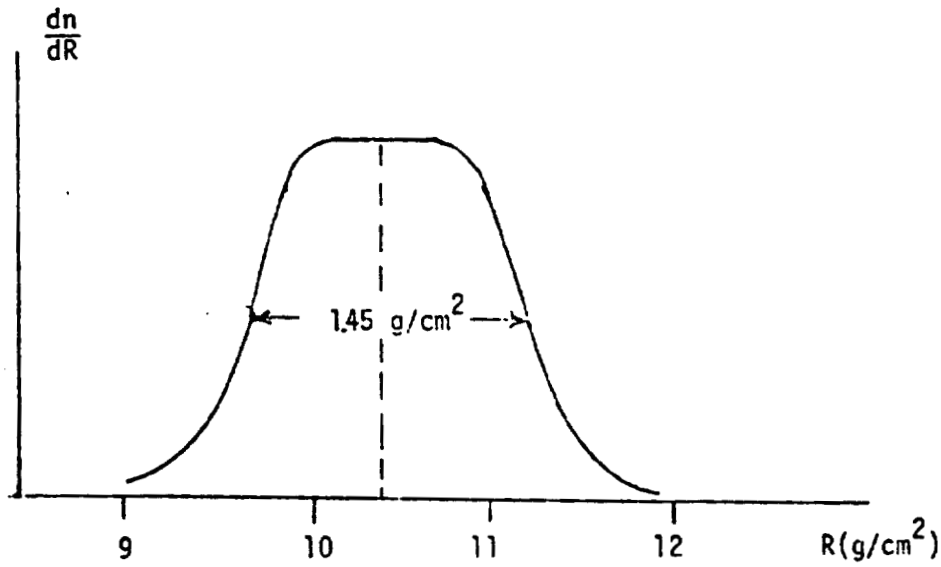

Fig. 2. APPROXIMATE LONGITUDINAL STOPPING DENSITY DISTRIBUTION OF NEGATIVE PIONS IN CARBON (T_{π^-} = 50 MeV, $\Delta p/p$ = 2.5%).

COPIED FOR
HS00132860.044

1093234

Fig. 3. ARRANGEMENT OF TARGETS, DETECTORS AND MULTIPLE SCATTERING REDUCTION FACTORS.

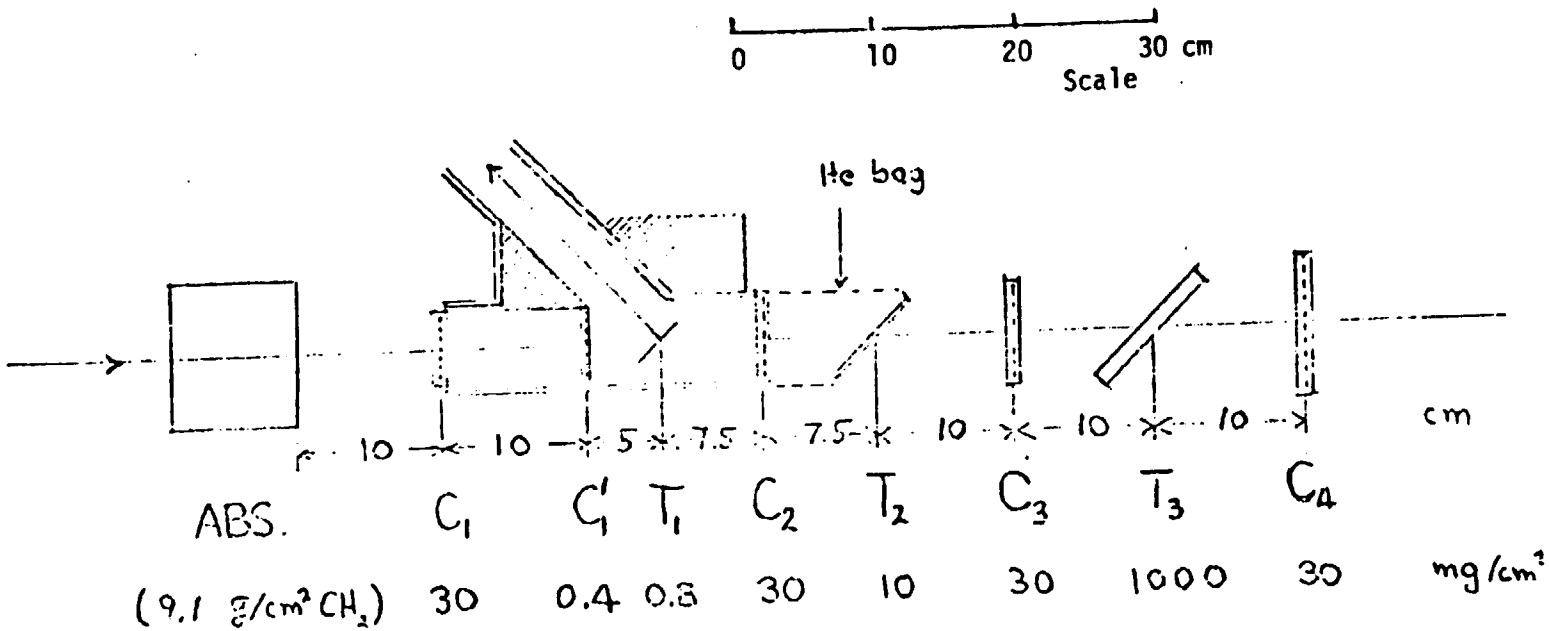

$\langle\theta^2\rangle$ REDUCTION FACTOR for:

Pions stopping in T_1	.26	.24	.22				
Pions stopping in T_2	.30	.25	.21	.16	.15		
Pions stopping in T_3	.33	.11	.072	.045	.030	.020	.015

COPIED FOR
HSPI 00132860.045

1093235

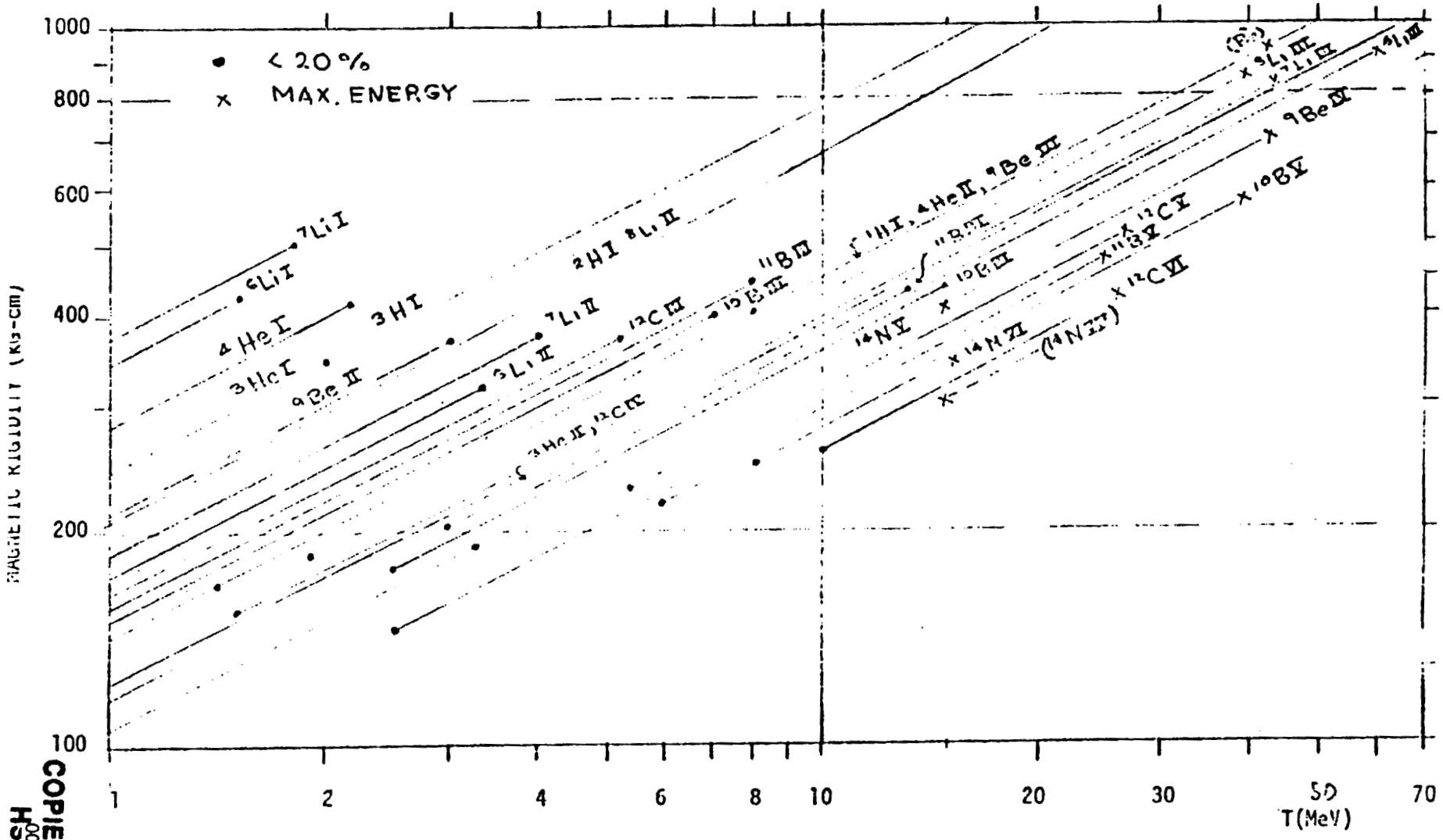

Fig. 4. MAGNETIC RIGIDITY OF FRAGMENTS VERSUS KINETIC ENERGY

COPIED FOR
HSRT
00132860.046

1093236

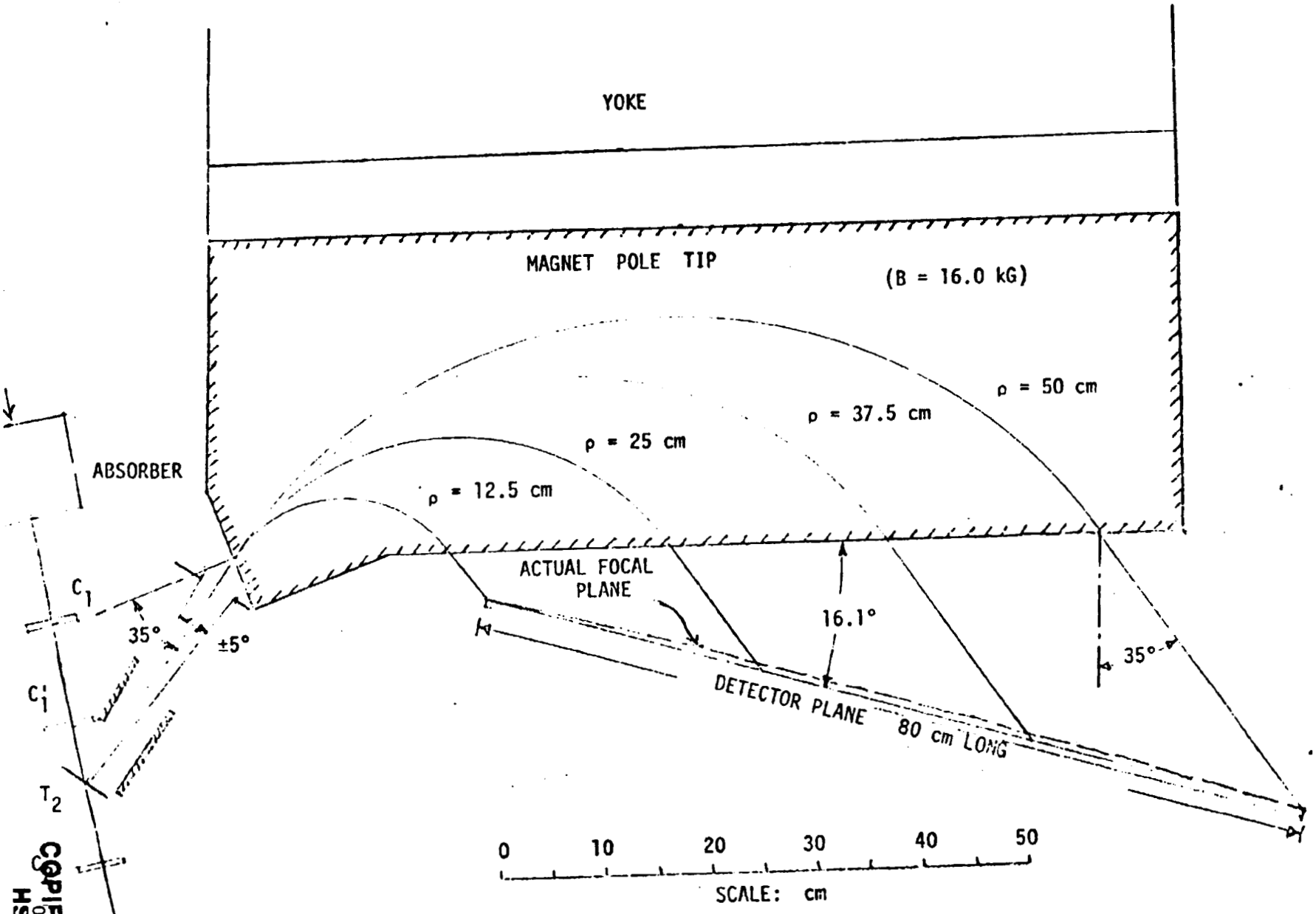

Fig. 5. COPENHAGEN MAGNET FOR LOW RANGE PARTICLES (Vacuum System not Indicated).

COPIED FOR
HSPT 0013286 0.047

1093237

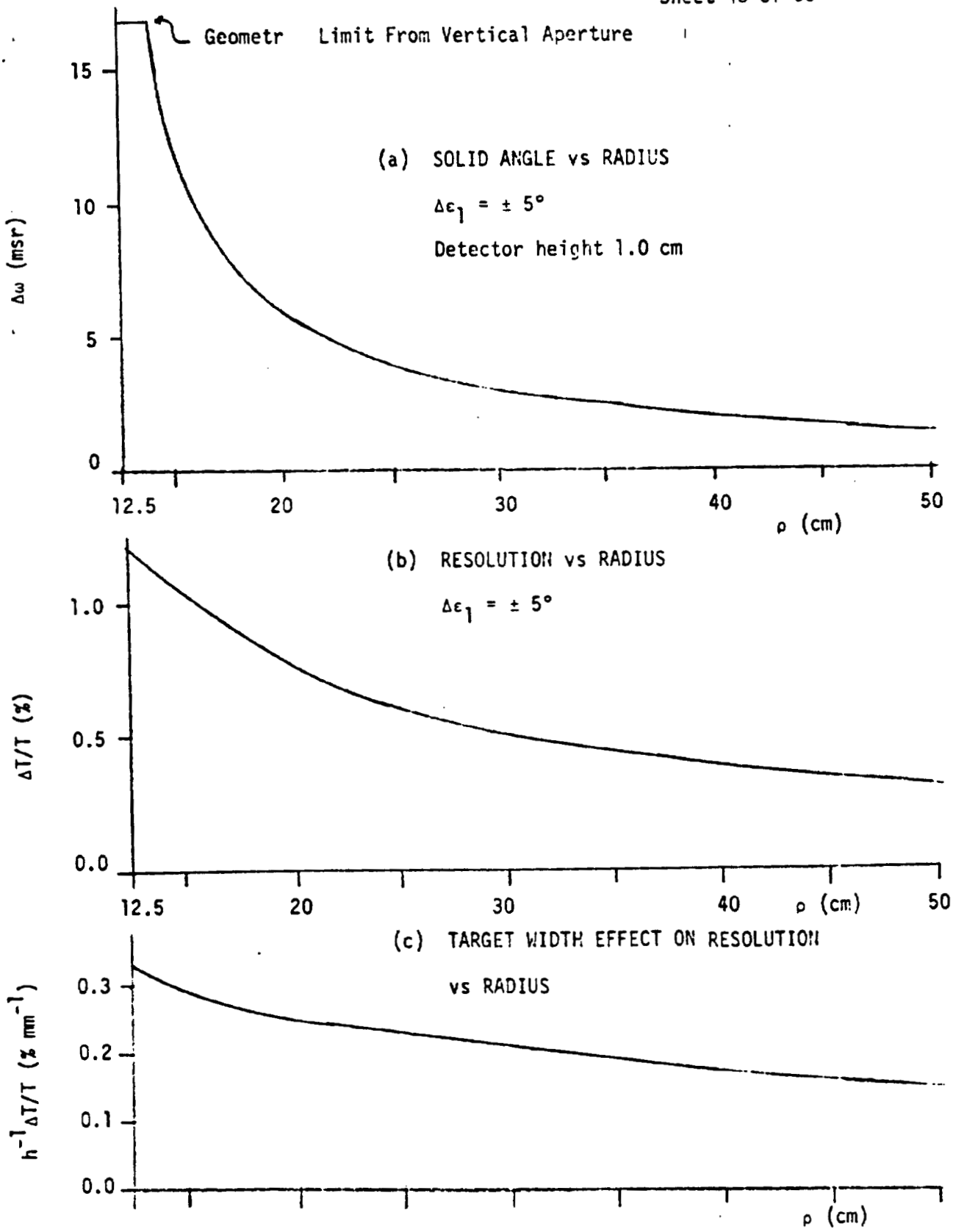

Fig. 6. PROPERTIES OF THE MAGNETIC SPECTROGRAPH

1093238

COPIE 00132860.048

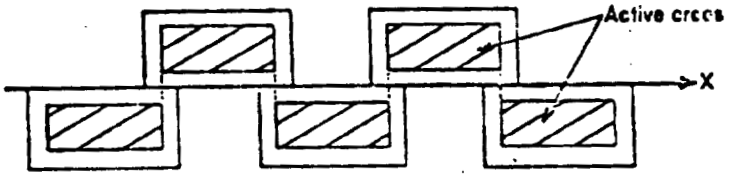

Fig. 7. ARRANGEMENT OF POSITION/ENERGY SENSITIVE DETECTORS

COPIED FOR HSPI
00132860.049

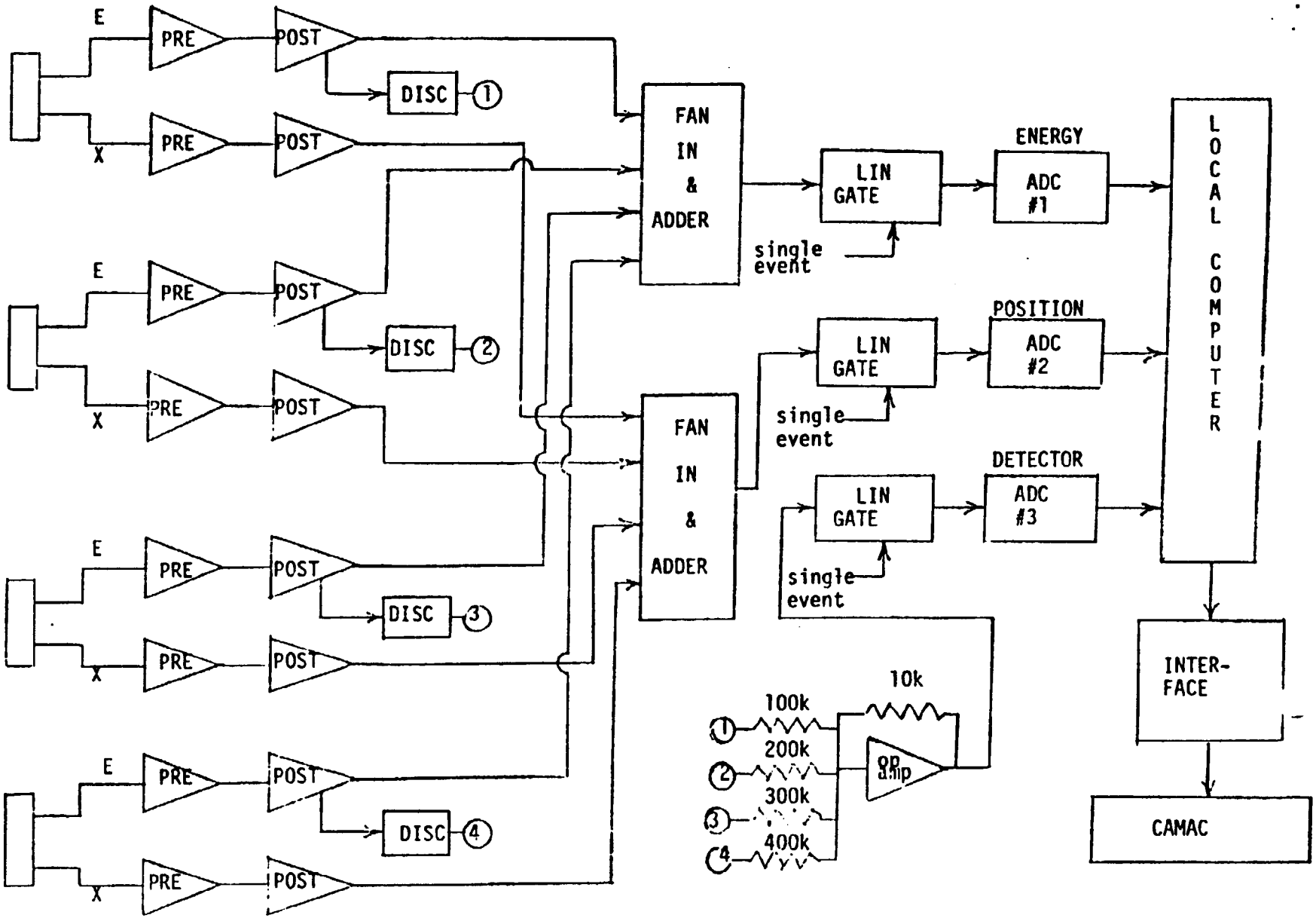

Fig. 8 SPECTROGRAPH ELECTRONICS

COPIED FOR
00132860.050
HSPT

1093240

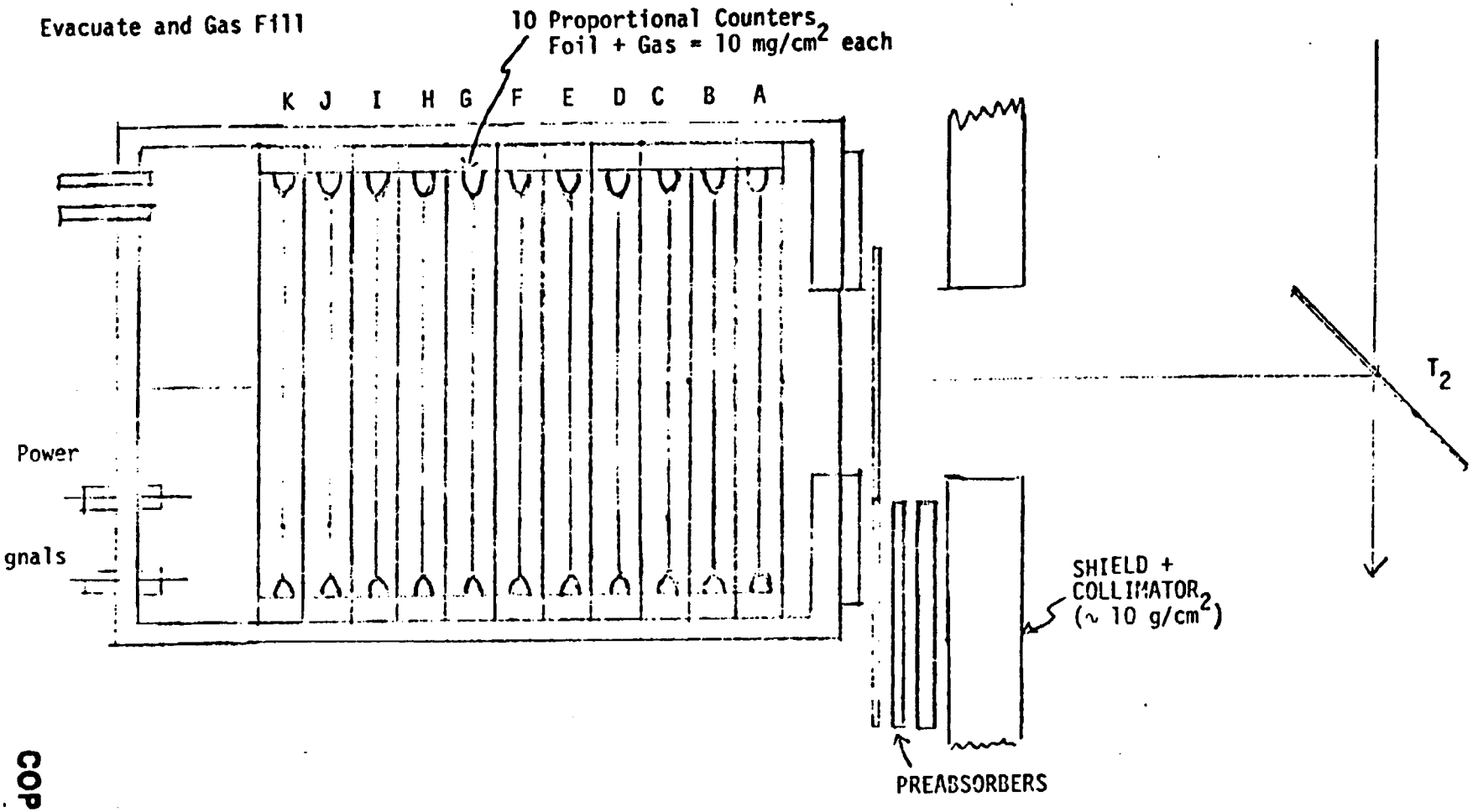

Fig. 9. RANGE CHAMBER Scale: Full Size

COP 00132860.051

1093241

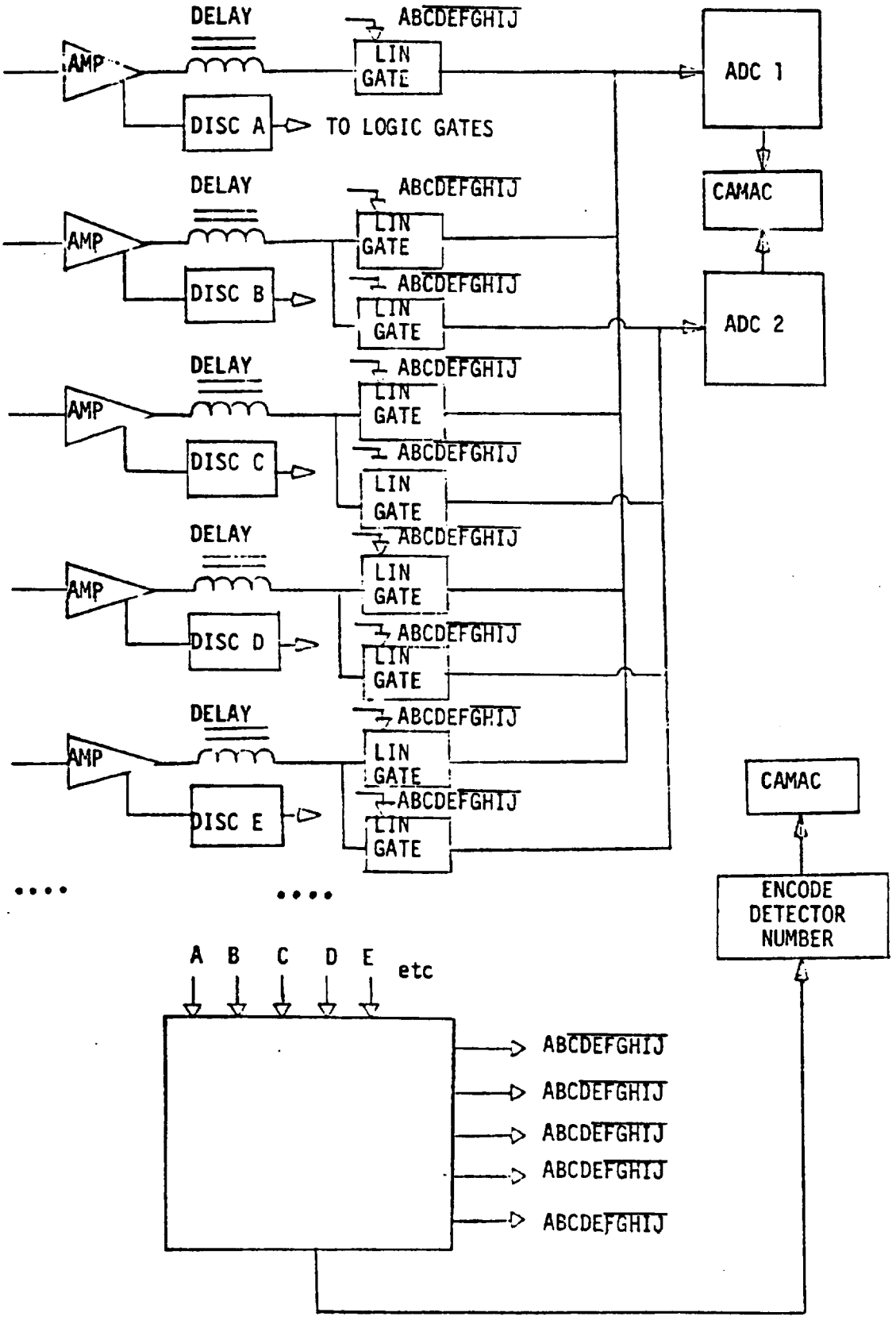

Fig. 10. DIFFERENTIAL RANGE CHAMBER ELECTRONICS

1093242

COPIED FOR
00132860.052

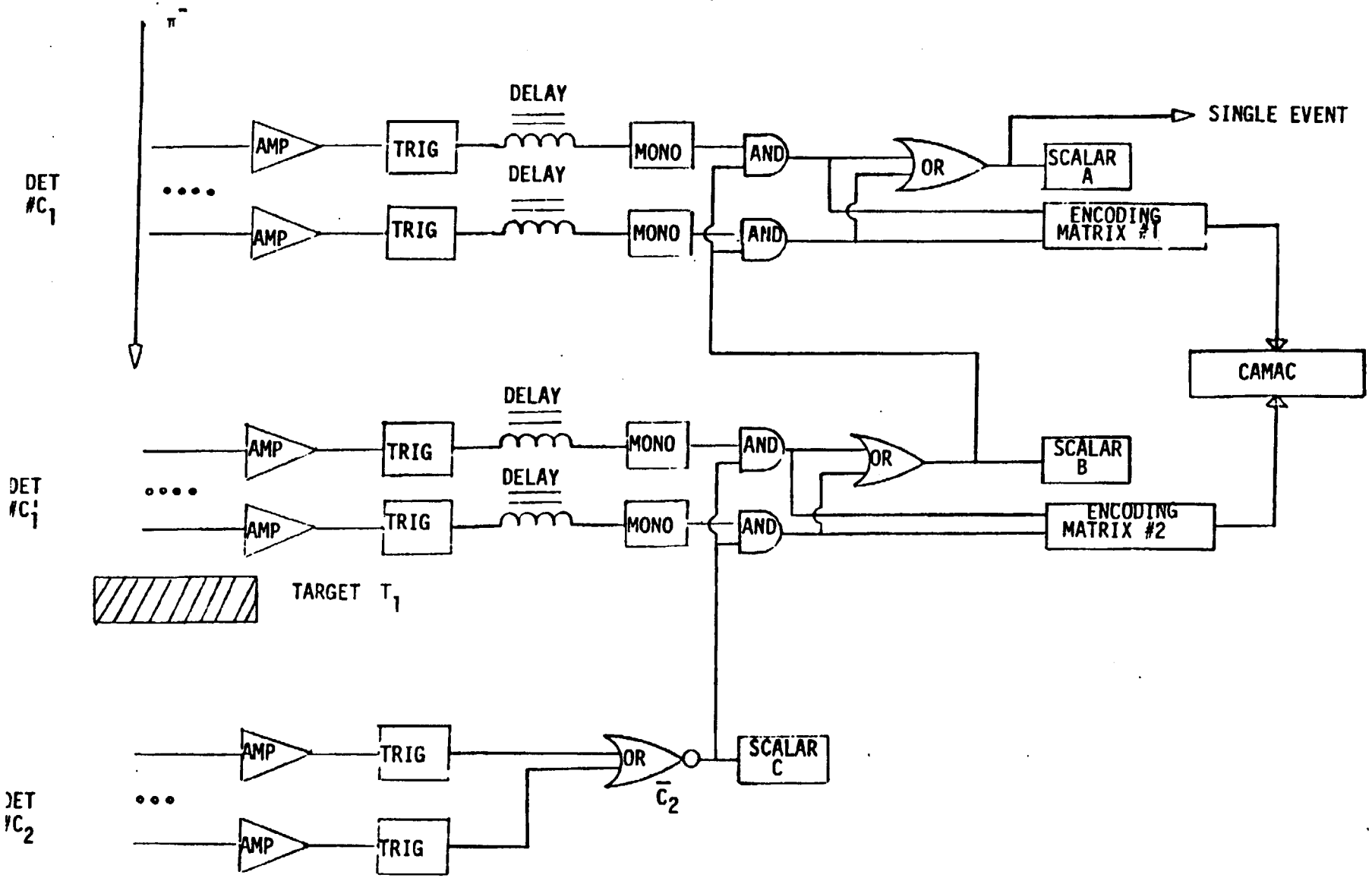

Fig. 11. MULTIWIRE DETECTORS ELECTRONICS

COPIED FOR
00132860.053
1093243

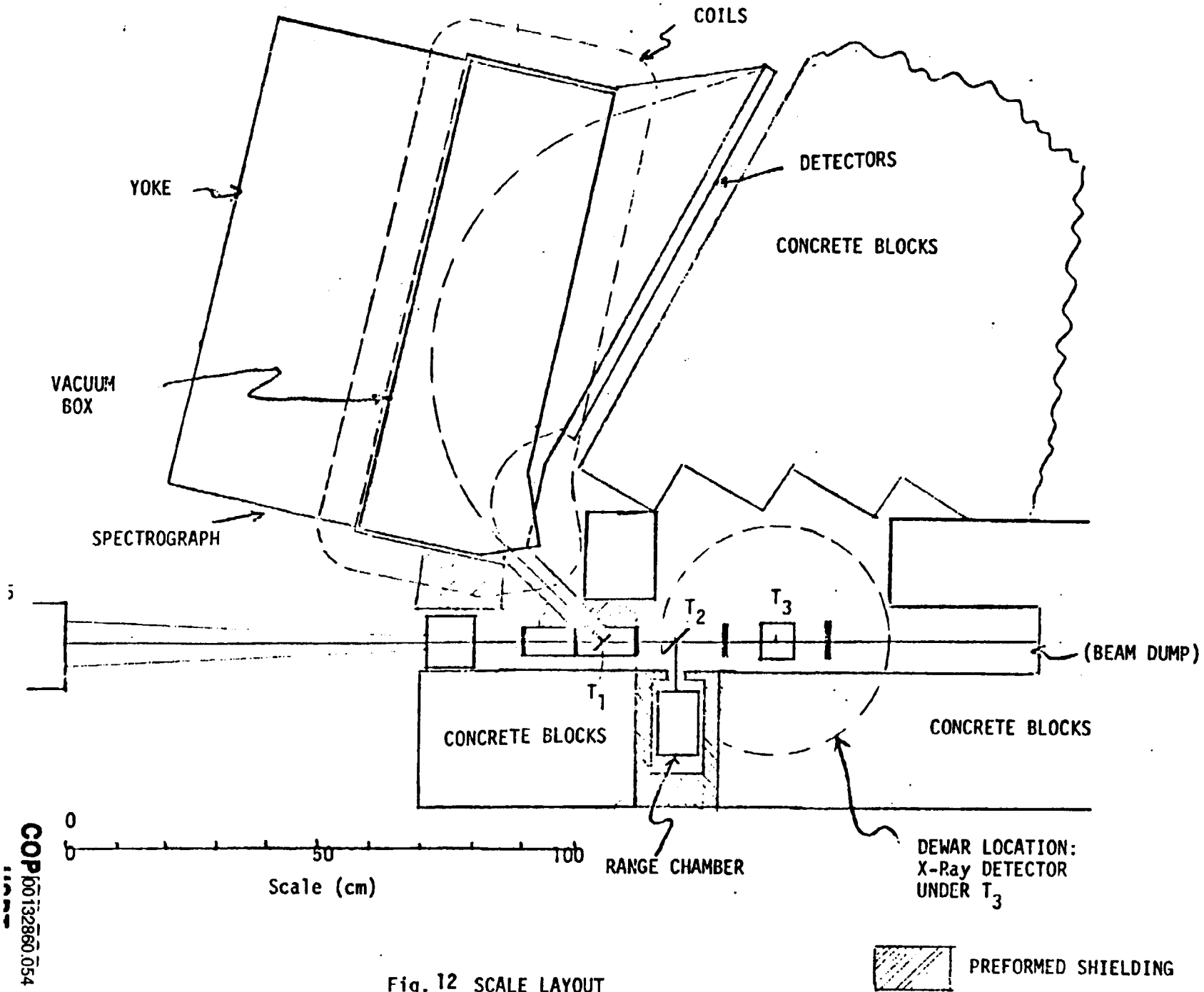

Fig. 12 SCALE LAYOUT

COP 00132860.054

1093244

SAFETY

Other than the routine hazards associated with high potentials on detectors, moving heavy equipment, etc., the only special hazards now apparent will arise from the fast neutron flux and the use of melamine targets.

1093245

COPIED FOR
00132860.055

APPLICATION FOR FINANCIAL SUPPORT

Because the present membership of the consortium is now entirely based in U. S. colleges and universities, it did not seem appropriate to request support from Canadian agencies at this time. Copies of this document are being sent to the National Research Council and the B. C. Cancer Institute as a matter of courtesy, and also, to the following governmental and private agencies within the U. S., as a preproposal.

U. S. Atomic Energy Commission, Division of Research

U. S. Atomic Energy Commission, Division of Biology and Medicine

National Science Foundation, Nuclear Physics Program

National Institute of Health, National Cancer Institute

American Cancer Society

1093246

COPIED FOR
H00132860.056